J. Fluid Mech. (2009), *vol.* 632, *pp.* 359–400.
doi:10.1017/S002211200900706X Printed in the United Kingdom

Critical bacterial concentration for the onset of collective swimming

GANESH SUBRAMANIAN[1]† AND DONALD L. KOCH[2]

[1]Engineering Mechanics Unit, Jawaharlal Nehru Centre for Advanced Scientific Research, Bangalore 560064, India

[2]School of chemical and bio-molecular engineering, Cornell University, Ithaca, NY 14853, USA

(Received 7 March 2008 and in revised form 4 March 2009)

We examine the stability of a suspension of swimming bacteria in a Newtonian medium. The bacteria execute a run-and-tumble motion, runs being periods when a bacterium on average swims in a given direction; runs are interrupted by tumbles, leading to an abrupt, albeit correlated, change in the swimming direction. An instability is predicted to occur in a suspension of 'pushers' (e.g. *E. Coli*, *Bacillus subtilis,* etc.), and owes its origin to the intrinsic force dipoles of such bacteria. Unlike the dipole induced in an inextensible fibre subject to an axial straining flow, the forces constituting the dipole of a pusher are directed outward along its axis. As a result, the anisotropy in the orientation distribution of bacteria due to an imposed velocity perturbation drives a disturbance velocity field that acts to reinforce the perturbation. For long wavelengths, the resulting destabilizing bacterial stress is Newtonian but with a negative viscosity. The suspension becomes unstable when the total viscosity becomes negative. In the dilute limit $(nL^3 \ll 1)$, a linear stability analysis gives the threshold concentration for instability as $(nL^3)_{crit} = ((30/C\mathscr{F}(r))(D_rL/U)(1 + 1/(6\tau D_r)))/(1-(15\mathscr{G}(r)/C\mathscr{F}(r))(D_rL/U)(1+1/(6\tau D_r)))$ for perfectly random tumbles; here, L and U are the length and swimming velocity of a bacterium, n is the bacterial number density, D_r characterizes the rotary diffusion during a run and τ^{-1} is the average tumbling frequency. The function $\mathscr{F}(r)$ characterizes the rotation of a bacterium of aspect ratio r in an imposed linear flow; $\mathscr{F}(r) = (r^2 - 1)/(r^2 + 1)$ for a spheroid, and $\mathscr{F}(r) \approx 1$ for a slender bacterium $(r \gg 1)$. The function $\mathscr{G}(r)$ characterizes the stabilizing viscous response arising from the resistance of a bacterium to a deforming ambient flow; $\mathscr{G}(r) = 5\pi/6$ for a rigid spherical bacterium, and $\mathscr{G}(r) \approx \pi/45(\ln r)$ for a slender bacterium. Finally, the constant C denotes the dimensionless strength of the bacterial force dipole in units of μUL^2; for *E. Coli*, $C \approx 0.57$. The threshold concentration diverges in the limit $((15\mathscr{G}(r)/C\mathscr{F}(r))(D_rL/U)(1 + 1/(6\tau D_r))) \rightarrow 1$. This limit defines a critical swimming speed, $U_{crit} = (D_rL)(15\mathscr{G}(r)/C\mathscr{F}(r))(1+1/(6\tau D_r))$. For speeds smaller than this critical value, the destabilizing bacterial stress remains subdominant and a dilute suspension of these swimmers therefore responds to long-wavelength perturbations in a manner similar to a suspension of passive rigid particles, that is, with a net enhancement in viscosity proportional to the bacterial concentration.

On the other hand, the stability analysis predicts that the above threshold concentration reduces to zero in the limit $D_r \rightarrow 0, \tau \rightarrow \infty$, and a suspension of non-interacting straight swimmers is therefore always unstable. It is then argued that the dominant effect of hydrodynamic interactions in a dilute suspension of

† Email address for correspondence: sganesh@jncasr.ac.in

such swimmers is via an interaction-driven orientation decorrelation mechanism. The latter arises from uncorrelated pair interactions in the limit $nL^3 \ll 1$, and for slender bacteria in particular, it takes the form of a hydrodynamic rotary diffusivity (D_r^h); for *E. Coli*, we find $D_r^h = 9.4 \times 10^{-5}(nUL^2)$. From the above expression for the threshold concentration, it may be shown that even a weakly interacting suspension of slender smooth-swimming bacteria ($r \gg 1$, $\mathscr{F}(r) \approx 1$, $\tau \to \infty$) will be stable provided $D_r^h > (C/30)(nUL^2)$ in the limit $nL^3 \ll 1$. The hydrodynamic rotary diffusivity of *E. Coli* is, however, too small to stabilize a dilute suspension of these swimmers, and a weakly interacting suspension of *E. Coli* remains unstable.

1. Introduction

Recent experiments (Wu *et al.* 2006) and simulations (Hernandez-Ortiz, Stolz & Graham 2005; Saintillan & Shelley 2007) have revealed the presence of increased velocity fluctuations in suspensions of swimming micro-organisms. Coherent vortical patterns have been observed on length scales exceeding the size of a single micro-organism (Wu & Libchaber 2000), implying that a suspension of bacteria swimming in an otherwise quiescent fluid may be an inherently unstable state at high concentrations. The above observations, in fact, point to the existence of collective swimming modes with long-ranged spatiotemporal correlations. In this paper, we show that a suspension of neutrally buoyant swimming bacteria (pushers) is indeed linearly unstable above a critical concentration.

A swimming bacterium, having the same density as the suspending fluid medium, does not exert a net force on the fluid, as must be the case from first principles; the head and tail of the bacterium therefore exert forces of equal magnitude in opposite directions, as it swims (see figure 1) (Berg 1983). Figure 2 illustrates the underlying physical mechanism of the instability. A passive particle such as a fibre tends to align along the extensional axis in an extensional flow; in this aligned state, the fibre, on account of its inextensibility, induces a disturbance velocity field that acts to retard the imposed flow. On the other hand, an active particle such as a slender *E. Coli* does align along the local extensional axis; but, for a weak imposed flow, for instance, a small amplitude velocity perturbation considered in the context of a linear stability analysis, the dominant effect in the aligned state is that of the velocity disturbance field arising from the intrinsic force dipole of the bacterium. Clearly, this disturbance flow field acts to reinforce the imposed extensional flow. One may therefore conceive of a situation where an imposed velocity perturbation alters the orientation distribution in a bacterial suspension such that the disturbance velocity field resulting from the anisotropy of the orientation distribution acts, on average, to reinforce the imposed disturbance. Thus, there is a mechanism for a positive feedback between orientation and velocity fluctuations, and an instability. Herein, we determine the critical concentration for the onset of this instability as a function of parameters that characterize the swimming motion of a single bacterium.

Earlier investigations on the occurrence of hydrodynamic instabilities in suspensions of micro-organisms have focused on gyrotactic micro-organisms, the algal species *C. nivalis* being an example. A suspension of such microscopic swimmers contained between horizontal boundaries becomes unstable owing to one of the two mechanisms. The first mechanism comes into play for relatively small separations between the boundaries. The gyrotactic torque causes the bottom-heavy algae to swim upward

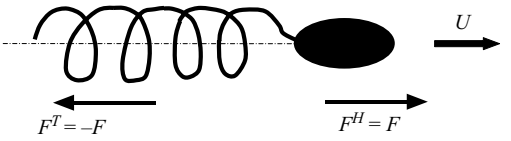

FIGURE 1. The figure shows an *E. Coli* (a 'pusher') together with the forces that it exerts on the fluid as it swims. The head exerts a force in the direction of swimming, dragging fluid along with it, while the tail rotates like a corkscrew to propel the head forward, in turn, pushing fluid behind; the symbols $\boldsymbol{F}^H$ and $\boldsymbol{F}^T$, respectively, denote the forces exerted on the fluid by the head and tail of the swimming bacterium.

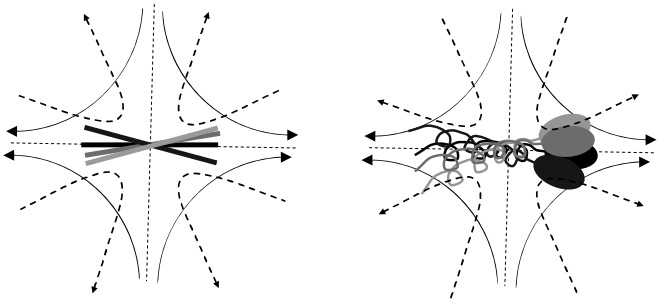

FIGURE 2. The figure shows the differing responses of a passive fibre and an active bacterium (a 'pusher') to an imposed extensional flow; the solid lines denote the imposed extensional flow, and the dashed lines the disturbance velocity field. The reinforcement in the case of the bacterium leads to an instability.

against gravity, rapidly leading to an unstable density stratification in the vertical direction since the algae are denser than water. The unstably stratified suspension is susceptible to the classical Rayleigh–Taylor overturning instability (see Chandrasekhar 1961; Childress, Levandowsky & Spiegel 1975). The stratification develops on a time scale of $O(H/U)$, where H is the separation between the boundaries, and U is a typical algal swimming speed. With increasing system size, however, the suspension is destabilized due to a second mechanism operating on a time scale shorter than $O(H/U)$. This mechanism operates in a homogeneous suspension, and involves a coupling of density and velocity perturbations. An imposed density perturbation causes alternating regions of upflow and downflow, and the resulting balance between the shear-induced and gyrotactic torques causes the algae to swim preferentially towards the denser regions. This reinforces the original density perturbation, and thereby results in an instability (see Pedley, Hill & Kessler 1988). In both the above instances, the origin of the instability is the density difference between the organism and the suspending medium. Heavy organisms with an asymmetric mass distribution swim in a preferred direction even in the absence of an imposed flow, and this directional swimming in a gravitational field leads to an instability.

On the other hand, bacteria such as *E. Coli* are much smaller in size, and have nearly the same density as water. One therefore expects any gravity-driven instability to be subdominant on length scales characterizing micro-fluidic experiments. Recent experimentalists with *E. Coli* have, however, observed the presence of increased fluctuations, and spatiotemporally coherent motions on scales larger than a single organism both in two-dimensional suspensions confined to a soap film (Wu & Libchaber 2000), and in three-dimensional suspensions (Soni *et al.* 2003; Wu *et al.*

2006). Experiments with concentrated suspensions of other bacteria such as *Bacillus subtilis* also report observations of coherent motions including high-speed jets and vortical patterns (see Mendelson *et al.* 1999; Dombrowski *et al.* 2004). In particular, Wu *et al.* (2006) have measured the translational diffusivities of *E. Coli* cells in a bacterial suspension, using a novel three-dimensional-defocused particle tracking method, as a means of characterizing the amplitude of velocity fluctuations in these systems. Trajectories analysed included those of the wild type *E. Coli* strain that exhibit a run-and-tumble behaviour, and mutants that do not tumble – the so-called smooth swimmers. In both instances, the measured translational diffusivities increased with increasing cell concentration; the diffusivities increased more rapidly in suspensions of smooth swimmers. This is in contrast to the expected trend in a stable system, wherein the first effects of interactions would serve to accelerate the orientation-decorrelation process in a swimming micro-organism; the resulting decrease in the correlation time would lead to a corresponding reduction in the translational diffusivity with increasing concentration. Recent simulations have also reported regimes of anomalous diffusion and coherent vortical structures in large populations of interacting swimmers (see Hernandez-Ortiz *et al.* 2005; Saintillan & Shelley 2007). It is worth noting that simulations thus far differ from experiments in having only modelled the dynamics of 'straight swimmers' wherein there are no intrinsic mechanisms for orientation decorrelation, and the orientation of a given swimmer changes only due to hydrodynamic interactions. In this paper, we suggest that the observed increased velocity fluctuations in both experiments and simulations of bacterial suspensions may be due to the onset of a hydrodynamic instability beyond a critical concentration. The analysis in the following sections determines this critical concentration. The critical concentration is, in fact, found to be lower for a suspension of smooth swimmers, implying that a suspension of such mutants is more easily destabilized, and tends to zero in the limit of straight swimmers. This is consistent with the findings of the above experiments and simulations.

The paper is organized as follows. The averaged equations governing the motion of the bacterial suspension are formulated in the next section, together with the underlying assumptions. The calculation of the threshold bacterial concentration from the linearized equations for the disturbance amplitudes is carried out in § 3 for a dilute bacterial suspension, where we also explain the underlying physical mechanism driving the instability. A threshold concentration arises because there exist orientation decorrelation mechanisms, for instance, rotary diffusion and tumbling, that limit the accumulation of the destabilizing bacterial stress driving the instability. The threshold concentration is thus determined as a function of a rotary diffusivity and a characteristic tumbling time. In the absence of hydrodynamic interactions, the rotary diffusion process models the orientation fluctuations resulting from imperfections in the propulsion mechanism; for instance, in *E. Coli*, a rotary diffusivity may be attributed to the fluctuations of the propelling flagellar bundle. In § 4, we argue that the dominant effect of hydrodynamic interactions in the dilute limit enters as an additional mechanism for orientation decorrelation. While for a bacterium of an arbitrary shape, a description of such a decorrelation mechanism will entail a non-local advection–diffusion equation in orientation space, for slender bacteria, the decorrelation process resulting from relatively weak pair interactions is shown to be a local diffusive one. The resulting hydrodynamic rotary diffusivity in this limit is then calculated from the dynamics of uncorrelated pair interactions. Interpreting the rotary diffusivity introduced in § 3 as being one solely due to hydrodynamic pair interactions, it is then shown that a suspension of weakly interacting smooth-swimming slender

bacteria remains unstable. Finally, in § 5, after summarizing the main results of the theoretical analysis in earlier sections, we discuss these predictions in the context of earlier theoretical efforts, recent experiments and simulations.

2. Governing equations

The averaged equations governing the motion of the bacterial suspension are

$$\nabla \cdot \langle \boldsymbol{u} \rangle = 0, \tag{2.1}$$

$$-\nabla \langle p \rangle + \mu \nabla^2 \langle \boldsymbol{u} \rangle + \nabla \cdot \langle \boldsymbol{\sigma}^B \rangle = \boldsymbol{0}, \tag{2.2}$$

where $\langle \boldsymbol{u} \rangle(\boldsymbol{x}, t)$ and $\langle p \rangle(\boldsymbol{x}, t)$ are the ensemble-averaged velocity and pressure fields, the angular brackets denoting the ensemble average, and the average is over all possible configurations of the bacterial suspension; a given configuration is specified by the instantaneous positions and orientations of all swimming bacteria in the suspension. In (2.2), μ is the viscosity of the suspending fluid medium, and $\langle \boldsymbol{\sigma}^B \rangle(\boldsymbol{x}, t)$ is an ensemble-averaged bacterial stress tensor. In writing down (2.1) and (2.2), we have assumed incompressibility and neglected inertial forces. The latter are of negligible importance on the length and time scales of interest. As a result, a quasi-steady approximation for the averaged equations is sufficient and memory effects associated with unsteady inertia are unimportant (in presence of unsteady inertial effects, a complete specification of an ensemble would, in principle, require the specification of all possible time trajectories leading up to the current configuration). Indeed, considering a typical example, that of a swimming *E. Coli*, one finds that the Reynolds number based on its swimming speed is $O(10^{-4})$. The details of the derivation of the above averaged equations are given in appendix A. The bacteria here are assumed to be neutrally buoyant, and their effect in the averaged equations appears therefore not as a net force, but rather as a stress field. The averaged bacterial stress $\langle \boldsymbol{\sigma}^B \rangle(\boldsymbol{x}, t)$ arises, in part, from the intrinsic force dipole associated with the swimming bacteria, and it is this intrinsic contribution that is responsible for the instability analysed in this paper. $\langle \boldsymbol{\sigma}^B \rangle(\boldsymbol{x}, t)$ equals the averaged density of force dipoles, and one finds (see appendix A)

$$\langle \boldsymbol{\sigma}^B \rangle(\boldsymbol{x}, t) = -n \int \mathrm{d}\boldsymbol{p}\ \Omega(\boldsymbol{x}, \boldsymbol{p}, t) \int_{-L/2}^{L/2} \mathrm{d}s\ \frac{1}{2} (\langle \boldsymbol{f}(s, t; \boldsymbol{x}, \boldsymbol{p}) \rangle_1 \boldsymbol{r} + \boldsymbol{r} \langle \boldsymbol{f}(s, t; \boldsymbol{x}, \boldsymbol{p}) \rangle_1), \tag{2.3}$$

where $\Omega(\boldsymbol{x}, \boldsymbol{p}, t)$ is the (normalized) probability density function for the spatial location $(\boldsymbol{x})$ and orientation $(\boldsymbol{p})$ of a single swimming bacterium, and n is the bacterial number density; thus, for N bacteria swimming within a volume V, $n = N/V$, and $\int (n\Omega)\, \mathrm{d}\boldsymbol{x}\, \mathrm{d}\boldsymbol{p} = N$. Further, $\langle \boldsymbol{f}(s, t; \boldsymbol{x}, \boldsymbol{p}) \rangle_1$ is the conditionally averaged linear force density exerted on the fluid by a swimming bacterium of length L and configuration $[\boldsymbol{x}, \boldsymbol{p}]$; the symbol $\langle . \rangle_1$ denotes a conditional ensemble average with the position and orientation of one bacterium specified. Here, s is an arclength coordinate with $s = \pm L/2$ denoting the ends of the bacterium, and $\boldsymbol{r} = s\boldsymbol{p}$ in (2.3) is the axial position relative to the geometric centre $(\boldsymbol{x})$ of the bacterium. The need for a conditional average arises because the force density on a given bacterium is a function of the local ambient flow, and the latter is determined, in part, by the disturbance velocity fields generated by neighbouring swimming bacteria. This situation is, of course, similar to a suspension of hydrodynamically interacting passive particles (see Kim & Karrila 1991). Thus, the average in $\langle \boldsymbol{f}(s, t; \boldsymbol{x}, \boldsymbol{p}) \rangle_1$ is over all possible configurations of the remaining $(N - 1)$ bacteria in the suspension. It is shown in appendix A that

$\langle \boldsymbol{f}(s,t;\boldsymbol{x},\boldsymbol{p})\rangle_1$ is given by the following expression:

$$\langle \boldsymbol{f}(s,t;\boldsymbol{x},\boldsymbol{p})\rangle_1 = \boldsymbol{f}^b(s;\boldsymbol{x},\boldsymbol{p}) + \frac{1}{(N-1)!}\int \Omega_{N-1|1}(C_{N-1},t|[\boldsymbol{x},\boldsymbol{p}])\boldsymbol{f}'(s;\boldsymbol{x},\boldsymbol{p};C_{N-1})\,\mathrm{d}C_{N-1}, \tag{2.4}$$

where we have used the abbreviated notation, $C_{N-1} \equiv [\boldsymbol{x}^\alpha, \boldsymbol{p}^\alpha]_{\alpha=1}^{N-1}$, for the bacterial configurations. In (2.4), $\boldsymbol{f}^b(s;\boldsymbol{x},\boldsymbol{p}) = \boldsymbol{f}^i(s;\boldsymbol{p}) + \boldsymbol{f}^e(s;\boldsymbol{x},\boldsymbol{p})$ is the linear force density exerted by an isolated bacterium with orientation $\boldsymbol{p}$ in the absence of interactions. Here, $\boldsymbol{f}^i(s;\boldsymbol{p})$ is the force density associated with the intrinsic force dipole, and is therefore a function of the particular species of bacterium, while $\boldsymbol{f}^e(s;\boldsymbol{x},\boldsymbol{p})$ is the force density induced by an imposed flow on account of the inextensibility of the bacterium (it is reasonable to regard a swimming bacterium as being inextensible in relatively weak flows); this latter contribution is one that exists even for passive particles on account of their rigidity, and gives rise to the familiar enhancement in viscosity of a dilute suspension of such particles. On the other hand, $\boldsymbol{f}'(s;\boldsymbol{x},\boldsymbol{p};C_{N-1})$ is the modification in this force density due to interactions with $(N-1)$ other bacteria in the volume V; the dependence of $\boldsymbol{f}'$ on the configuration of the bacterium of interest ($[\boldsymbol{x},\boldsymbol{p}]$), and the configurations of the remaining bacteria in the suspension (C_{N-1}) have been indicated separately. The statistics of the configurations are governed by suitably normalized probability density functions in phase (position–orientation) space. In (2.4), $\Omega_{N-1|1}(C_{N-1},t|[\boldsymbol{x},\boldsymbol{p}])$ is the conditional probability density governing the configurations of $(N-1)$ other bacteria given the configuration of a single bacterium $[\boldsymbol{x},\boldsymbol{p}]$, while $\Omega(\boldsymbol{x},\boldsymbol{p},t)$ is, as before (see (2.3)), the singlet probability density. With the neglect of inertia, both $\boldsymbol{f}^b$ and $\boldsymbol{f}'$ are completely determined by the instantaneous configurations and velocities of the swimming bacteria, and the time dependence in the averaged force density arises solely from the time dependence of the probability density functions. The latter satisfy suitable kinetic equations; the equation governing the evolution of $\Omega(\boldsymbol{x},\boldsymbol{p},t)$ appears below. Finally, we observe that the swimming bacteria are torque free, and accordingly, $\langle \boldsymbol{\sigma}^B\rangle$ given by (2.3) and (2.4) is symmetric.

In order to write down an equation governing the singlet probability density, $\Omega(\boldsymbol{x},\boldsymbol{p},t)$, the neutrally buoyant bacteria are assumed to execute a run-and-tumble motion. During a run, a bacterium swims with speed U, parallel to its orientation $\boldsymbol{p}$, which varies slowly as a result of a weak rotary diffusion. Thus, even in a run, there is a gradual decorrelation in orientation on a time scale of $O(D_r^{-1})$, D_r being the rotary diffusivity. The need for a rotary diffusivity arises because experimental observations have shown that the path of a bacterium during a run is not a straight line (see Berg 1983). A rotary diffusion, superimposed on translation along $\boldsymbol{p}$, is therefore used to model this deviation from linearity. It is worth noting that, even in the limit of small concentrations when effects related to hydrodynamic interactions between bacteria are negligible, the rotary diffusion may not be the result of Brownian motion. For the case of *E. Coli*, the rotary Brownian diffusivity calculated using the total length of the bacterium (≈ 10 microns) turns out to be much smaller than that estimated using typical trajectories obtained from experiments (see Berg 1983). It is therefore likely, at least for *E. Coli*, that the observed deviations from a rectilinear trajectory during a run are not due to thermal forces, but rather due to imperfections in the motion of the flagella constituting the propelling helical bundle. A further indication of the importance of D_r comes from the experimental observation of Wu *et al.* (2006) that even smooth-swimming bacteria undergo a translational diffusion for long times owing

to the coupled effects of swimming and rotary diffusion. The translational diffusivity for such swimmers would be divergent in the dilute limit (negligible interactions) if D_r were to be identically zero. The translational diffusivity of smooth swimmers was, in fact, observed to be about 10 times larger than that of bacteria that run and tumble. The bacterial concentration in these experiments was high enough for the rotary diffusion to also include a contribution due to hydrodynamic interactions. It is shown in § 4 that, in a dilute suspension of slender bacteria, the effect of pair-hydrodynamic interactions on sufficiently long time scales, on the orientation of a single swimming bacterium, may indeed be accounted for by a hydrodynamic rotary diffusivity.

The gradual changes in orientation due to rotary diffusion during runs are interspersed with tumbles, short episodes of erratic motion that lead to a sudden, and a rather large, change in orientation. The tumbling events may be regarded as instantaneous, as is typically the case for bacteria; for instance, for *E. Coli*, the duration of a run (τ) is anywhere from 1 to 4 s, while the tumble mode persists only for about 0.1 s. The statistics of the instantaneous tumbles are well approximated by a Poisson process with frequency τ^{-1}. We also allow for a non-trivial correlation between the pre-tumble and post-tumble orientations. A perfectly random tumble would imply a mean orientation change of 90°; the average change in orientation for *E. Coli* is about 68.5°, indicating a correlation in the forward direction (see Berg 1983). With the above assumptions, $\Omega(\boldsymbol{x}, \boldsymbol{p}, t)$ satisfies

$$\frac{\partial \Omega}{\partial t} + (U\boldsymbol{p} + \boldsymbol{u}) \cdot \nabla_x \Omega + \nabla_p \cdot (\dot{\boldsymbol{p}}\, \Omega) - D_r \nabla_p^2\, \Omega + \frac{1}{\tau}\left(\Omega - \int K(\boldsymbol{p}|\boldsymbol{p}') \Omega(\boldsymbol{x}, \boldsymbol{p}', t)\, \mathrm{d}\boldsymbol{p}' \right) = 0, \tag{2.5}$$

where ∇_p is the gradient operator over the unit sphere; in spherical polar coordinates, $\nabla_p = \mathbf{1}_\theta \partial/\partial\theta + \mathbf{1}_\phi (1/\sin\theta)(\partial/\partial\phi)$. According to (2.5), for a force-free bacterium that swims with velocity $U\boldsymbol{p}$ and is, in addition, convected by the fluid velocity field $\boldsymbol{u}$, Ω along the resulting trajectory changes due to rotary diffusion, tumbling and a rotation ($\dot{\boldsymbol{p}}$) by the ambient flow field. The ambient flow includes the disturbance velocity fields due to neighbouring swimming bacteria, and one may therefore split the total rotation into one by an imposed flow ($\dot{\boldsymbol{p}}^\infty$) and one due to interactions ($\dot{\boldsymbol{p}}^i$); thus

$$\dot{\boldsymbol{p}}(\boldsymbol{x}, t) = \dot{\boldsymbol{p}}^\infty(\boldsymbol{x}, t) + n \int \dot{\boldsymbol{p}}^i(\boldsymbol{x}|C_{N-1}) \Omega_{N-1|1}(C_{N-1}, t|\boldsymbol{x}, \boldsymbol{p})\, \mathrm{d}C_{N-1}, \tag{2.6}$$

Further, observe that (2.5) is an evolution equation, and therefore describes a Markov process. This is because the statistics of the tumbling events have been modelled by a Poisson process. The probability that a tumble occurs in an infinitesimal interval of time $\mathrm{d}t$ remains the same, being proportional to $\mathrm{d}t/\tau$, independent of any earlier tumbling events. With this assumption, the impulsive effect of tumbling on the orientation distribution may be regarded as that of a linear collision process. Thus, in a manner similar to the Boltzmann equation for gases (see Chapman & Cowling 1991), one would have a change in the probability on account of both 'direct' and 'inverse' events; the former denote a decrease in probability due to a tumble that causes a bacterium to leave the phase space interval of interest ($\mathrm{d}\boldsymbol{x}, \mathrm{d}\boldsymbol{p}$), while the latter represent the increment in probability due to all tumbling events that lead to the final orientation of the bacterium lying in the aforementioned interval. For a Poisson process, the effect of the direct events is simply given by Ω/τ. The inverse events have been modelled in (2.5) by a transition probability $K(\boldsymbol{p}\,|\boldsymbol{p}')$; $K(\boldsymbol{p}\,|\boldsymbol{p}')$ is thus the (conditional) probability density associated with an orientation jump (tumble) from $\boldsymbol{p}'$ to $\boldsymbol{p}$, given that the pre-tumble orientation is $\boldsymbol{p}'$. Thus, $K(\boldsymbol{p}|\boldsymbol{p}')$

determines the decorrelation accompanying a tumble; conservation of probability implies $\int K(\boldsymbol{p}|\boldsymbol{p}')\,\mathrm{d}\boldsymbol{p} = \int K(\boldsymbol{p}|\boldsymbol{p}')\,\mathrm{d}\boldsymbol{p}' = 1$. We choose $K(\boldsymbol{p}|\boldsymbol{p}') = (\beta/4\pi\sinh\beta)\,\mathrm{e}^{\beta(\boldsymbol{p}\cdot\boldsymbol{p}')}$, a simple form consistent with the aforementioned constraints, and where the parameter β measures the correlation between the pre- and post-tumble orientations; so, for $\beta \to 0$, $K = 1/4\pi$, corresponding to perfectly random tumbles, while in the limit $\beta \to \infty$, each tumble only leads to an infinitesimally small change in orientation. The value of β for a particular bacterium species may be determined from known statistical measures characterizing the tumbling events. Again, for the case of *E. Coli*, the mean change in orientation accompanying a tumble ($\langle\theta\rangle$) is about 68.5° (see Berg 1983). With the above form for $K(\boldsymbol{p}|\boldsymbol{p}')$, $\langle\theta\rangle = (\beta/2\sinh\beta)\int_0^\pi \mathrm{e}^{\beta\cos\theta}(\theta\sin\theta)\,\mathrm{d}\theta$, and the required average value is obtained for $\beta \approx 1$. We also observe from (2.5) that the bacteria are smooth swimmers in the limit $\tau \to \infty$ with orientational decorrelation occurring on account of rotary diffusion, and due to hydrodynamic interactions on longer time scales (see § 4). Finally, we note that, similar to $\dot{\boldsymbol{p}}$, the velocity field $\boldsymbol{u}$ in (2.5) may include both an imposed flow and the disturbance velocity fields due to neighbouring bacteria. One may therefore write $\boldsymbol{u}$ in the form

$$\boldsymbol{u}(\boldsymbol{x},t) = \boldsymbol{u}^\infty(\boldsymbol{x},t) + n\int \boldsymbol{u}^i(\boldsymbol{x}|C_{N-1})\Omega_{N-1|1}(C_{N-1},t|\boldsymbol{x},\boldsymbol{p})\,\mathrm{d}C_{N-1}, \tag{2.7}$$

where $\boldsymbol{u}^\infty(\boldsymbol{x},t)$ denotes an imposed flow field, and $\boldsymbol{u}^i(\boldsymbol{x}|C_{N-1})$ is the disturbance velocity field at the location of the given bacterium for a configuration C_{N-1} of the $(N-1)$ other bacteria.

Writing down the governing averaged equations for the motion of a bacterial suspension, now in their expanded form, one obtains

$$\nabla\cdot\langle\boldsymbol{u}\rangle = 0, \tag{2.8}$$

$$\begin{aligned}-\nabla\langle p\rangle + \mu\nabla^2\langle\boldsymbol{u}\rangle = n\nabla\cdot\Bigg(\int \mathrm{d}\boldsymbol{p}\;\Omega(\boldsymbol{x},\boldsymbol{p},t)\Bigg[\int_{-L/2}^{L/2}\mathrm{d}s\;\frac{1}{2}(\boldsymbol{f}^b(s;\boldsymbol{x},\boldsymbol{p})(s\boldsymbol{p}) + (s\boldsymbol{p})\boldsymbol{f}^b(s;\boldsymbol{x},\boldsymbol{p}))\\ + \int_{-L/2}^{L/2}\mathrm{d}s\;\frac{1}{2}\Bigg\{\Bigg(\frac{1}{(N-1)!}\int \Omega_{N-1|1}\boldsymbol{f}'(s;\boldsymbol{x},\boldsymbol{p};C_{N-1})\,\mathrm{d}C_{N-1}\Bigg)(s\boldsymbol{p})\\ + (s\boldsymbol{p})\Bigg(\frac{1}{(N-1)!}\int \Omega_{N-1|1}\boldsymbol{f}'(s;\boldsymbol{x},\boldsymbol{p};C_{N-1})\,\mathrm{d}C_{N-1}\Bigg)\Bigg\}\Bigg]\Bigg),\end{aligned} \tag{2.9}$$

$$\begin{aligned}&\frac{\partial\Omega}{\partial t} + (U\boldsymbol{p} + \boldsymbol{u}^\infty + n\int \boldsymbol{u}^i(\boldsymbol{x}|C_{N-1})\Omega_{N-1|1}\mathrm{d}C_{N-1})\cdot\nabla_x\Omega\\ &+\nabla_p\cdot\Bigg(\Bigg\{\dot{\boldsymbol{p}}^\infty(\boldsymbol{x},t) + n\int \dot{\boldsymbol{p}}^i(\boldsymbol{x}|C_{N-1})\Omega_{N-1|1}\mathrm{d}C_{N-1}\Bigg\}\Omega\Bigg)\\ &- D_r\nabla_p^2\,\Omega + \frac{1}{\tau}\Bigg(\Omega - \int K(\boldsymbol{p}|\boldsymbol{p}')\Omega(\boldsymbol{x},\boldsymbol{p}',t)\,\mathrm{d}\boldsymbol{p}'\Bigg) = 0.\end{aligned} \tag{2.10}$$

The system of equations for $\langle\boldsymbol{u}\rangle$, $\langle\boldsymbol{p}\rangle$ and Ω is evidently not a closed one. Both the equations of motion (via the bacterial force density $\boldsymbol{f}'$) and the kinetic equation for the singlet probability density depend on $\Omega_{N-1|1}(C_{N-1},t|\boldsymbol{x},\boldsymbol{p})$, and one therefore needs to know the statistics of multi-bacterial interactions. It is well-known from the averaged-equation approach for viscous suspensions (see Hinch 1977) that one may make analytical progress in the dilute limit by considering the multi-bacterial hydrodynamic interactions in a sequential manner (pairs, triplets, etc.). This leads to what, in principle,

is an infinite hierarchy of averaged equations with higher-order conditional averages appearing at succeeding orders in n. Truncation of the hierarchy at any given order leads to a statistical description accurate to the corresponding order in n; for instance, a pair interaction scenario accurate to $O(n^2)$ is obtained by neglecting terms involving probability density functions conditioned on the configurations of two or more bacteria.

In this section and the next, where we carry out the stability analysis, we shall restrict ourselves to the lowest order approximation by neglecting any correlations between the positions and orientations of the different swimming bacteria, an approximation valid in the dilute limit. This is equivalent to replacing the conditional averages in both the equations of motion and in the kinetic equation for the singlet probability density by the corresponding unconditional averages. The resulting simplified equations may be regarded as a mean-field approximation. In the absence of an imposed flow, a bacterium now rotates due to the mean velocity gradient produced by the disturbance velocity fields of other bacteria whose orientations and positions remain unaffected by the velocity disturbance due to the given bacterium. Such a mean-field treatment is only possible because the velocity disturbance due to each bacterium is long ranged decaying only as $O(1/x^2)$ with distance x from the bacterium; as a result, the average velocity field in the vicinity of a given bacterium is dominated by slowly varying contributions arising from the large number of bacteria in the far field rather than the small rapidly fluctuating contributions of neighbouring bacteria at distances of the order of its own size. As already indicated earlier, the effect of these distant bacteria may be regarded in terms of a stress field, and the mean velocity field experienced by a given bacterium in the absence of an imposed flow therefore results from slowly varying long-wavelength anisotropic fluctuations in the effective stress field associated with a bacterial suspension. In the context of a linear stability analysis pertaining to the length and time scales characterizing the motion of a single bacterium, the aforementioned slow fluctuations may then be treated as imposed perturbations. This equivalence of the unconditional mean fields to 'imposed' long-wavelength perturbations allows one to analyse the intrinsic instability of a bacterial suspension due to long-ranged hydrodynamic interactions via a traditional stability analysis involving the response of a quiescent suspension to an imposed perturbation.

The governing equations in the mean-field approximation may now be obtained from by first splitting the conditional averages in (2.8)–(2.10) into an unconditional average, the mean-field and a contribution arising from pair-correlations due to hydrodynamic interactions (see appendix A). The former only allows for the correlation of a bacterium orientation with its own (absolute) position in the mean field; this then leads to extended spatial domains with correlated orientations in the primary mode of instability (see § 3). The latter contribution considers hydrodynamically induced correlations in the orientations of a pair of bacteria as a function of their relative position, an effect that is expected to remain small in the dilute limit. Thus, in the absence of an external flow, the total force density in (2.4) may be written as

$$\langle \boldsymbol{f}(s,t;\boldsymbol{x},\boldsymbol{p})\rangle_1 = \hat{\boldsymbol{f}}^b(s;\boldsymbol{x},\boldsymbol{p}) + \frac{1}{(N-1)!}\int \Omega'_{N-1|1}(C_{N-1},t|[\boldsymbol{x},\boldsymbol{p}])\boldsymbol{f}'(s;\boldsymbol{x},\boldsymbol{p};C_{N-1})\,\mathrm{d}C_{N-1}, \quad (2.11)$$

where $\hat{\boldsymbol{f}}^b = \boldsymbol{f}^i(s;\boldsymbol{p}) + \boldsymbol{f}^m(s;\boldsymbol{x},\boldsymbol{p})$ with $\boldsymbol{f}^m(s;\boldsymbol{x},\boldsymbol{p}) = (1/(N-1)!)\int \Omega_{N-1}(C_{N-1},t)\,\boldsymbol{f}'(s;\boldsymbol{x},\boldsymbol{p};C_{N-1})\mathrm{d}C_{N-1}$ being the force density arising from the mean field; the average

in the second term in (2.11) is now based on $\Omega'_{N-1|1}$, the perturbation in the conditional probability density from its uncorrelated value, and is clearly $O(n)$ for $n \to 0$. In a similar manner, one may, in the absence of an imposed flow, approximate the velocity field $\boldsymbol{u} = \int \boldsymbol{u}^i(\boldsymbol{x}|C_{N-1})\Omega_{N-1|1}\mathrm{d}C_{N-1}$ in (2.10) by a mean-field convection ($\boldsymbol{u}^m$) of the singlet probability density Ω, and $\int \dot{\boldsymbol{p}}^i(\boldsymbol{x}|C_{N-1})\mathrm{d}C_{N-1}$ in the same equation by the rotation of a given bacterium due to the gradient associated with the mean field ($\dot{\boldsymbol{p}}^m$). The additional contributions arising from pair-correlations will again be proportional to $\Omega'_{N-1|1}$, and may be neglected. Further, dropping the averaging brackets (now denoting the unconditional averages) for notational simplicity, system of equations (2.8)–(2.10) reduces to the following simpler form in the mean-field approximation:

$$\nabla \cdot \boldsymbol{u}^m = 0, \tag{2.12}$$

$$-\nabla p + \mu \nabla^2 \boldsymbol{u}^m = n\nabla \cdot \left(\int \mathrm{d}\boldsymbol{p}\, \Omega(\boldsymbol{x}, \boldsymbol{p}, t) \int_{-L/2}^{L/2} \mathrm{d}s\, \frac{1}{2} (\hat{\boldsymbol{f}}^b(s; \boldsymbol{x}, \boldsymbol{p})(s\boldsymbol{p}) + (s\boldsymbol{p})\hat{\boldsymbol{f}}^b(s; \boldsymbol{x}, \boldsymbol{p})) \right), \tag{2.13}$$

$$\frac{\partial \Omega}{\partial t} + (U\boldsymbol{p} + \boldsymbol{u}^m) \cdot \nabla_x \Omega + \nabla_p \cdot (\dot{\boldsymbol{p}}^m \Omega) - D_r \nabla_p^2 \Omega + \frac{1}{\tau} \left(\Omega - \int K(\boldsymbol{p}|\boldsymbol{p}') \Omega(\boldsymbol{x}, \boldsymbol{p}', t)\, \mathrm{d}\boldsymbol{p}' \right) = 0. \tag{2.14}$$

We note from comparing the above set of equations with original system (2.8)–(2.10) that the difference between the velocity field in the equations of continuity and motion, and that in the kinetic equation (wherein both the translational and rotational convections must not include the direct effect of the test bacterium), becomes vanishingly small for large N in the coarse-grained mean-field approximation. Using $\hat{\boldsymbol{f}}^b(s; \boldsymbol{x}, \boldsymbol{p}) = \boldsymbol{f}^i(s; \boldsymbol{p}) + \boldsymbol{f}^m(s; \boldsymbol{x}, \boldsymbol{p})$, we observe that, in the absence of inertia, the force density associated with the intrinsic dipole, $\boldsymbol{f}^i(s; \boldsymbol{p})$, must be proportional to μU. Assuming an axial force density, we have $\boldsymbol{f}^i(s, \boldsymbol{p}) \propto f^i(s/L)(\mu U \boldsymbol{p})$, where $f^i(s/L)$ is a dimensionless scalar function denoting the detailed spatial dependence of the force density. Further, using this form in the right-hand side of (2.13), the term representing the bacterial stress tensor $\boldsymbol{\sigma}^B$, in a dilute suspension, may be written as the sum of active (swimming) and passive contributions, where the former is now in the form of an orientationally averaged stress (see Simha & Ramaswamy 2002). Thus,

$$\boldsymbol{\sigma}^B = -C(n\mu U L^2) \int \mathrm{d}\boldsymbol{p}\, \Omega(\boldsymbol{x}, \boldsymbol{p}, t) \left(\boldsymbol{pp} - \frac{1}{3}\boldsymbol{\delta} \right) \mathrm{d}\boldsymbol{p} - n \int \mathrm{d}\boldsymbol{p}\, \Omega(\boldsymbol{x}, \boldsymbol{p}, t) \int_{-L/2}^{L/2} \mathrm{d}s\, \frac{1}{2} (\boldsymbol{f}^m(s; \boldsymbol{x}, \boldsymbol{p})(s\boldsymbol{p}) + (s\boldsymbol{p})\boldsymbol{f}^m(s; \boldsymbol{x}, \boldsymbol{p})). \tag{2.15}$$

The constant of proportionality C in the first term is determined by $f^i(s/L)$; specifically, $C = \int_{-1/2}^{1/2} \hat{s} f^i(\hat{s})\, \mathrm{d}\hat{s}$ with $\hat{s} = s/L$. Note that $C > 0$ for pushers, and $C < 0$ for pullers. An expression for the linear force density, and thence, the value of C, for a slender bacterium like *E. Coli* has been calculated elsewhere (see Liao *et al.* 2007); this will be used later in § 3 when obtaining a quantitative estimate for the threshold concentration for instability in a suspension of *E. Coli*. Also note that in (2.15) we have defined the active component of $\boldsymbol{\sigma}^B$ to be traceless without loss of generality, since an isotropic bacterial stress may be balanced by a modified pressure field in (2.2).

Using the simplified form for $\boldsymbol{\sigma}^B$ from (2.15), the system of averaged equations governing the motion of a dilute bacterial suspension, now written in index notation,

is given by

$$\frac{\partial u_i}{\partial x_i} = 0, \tag{2.16}$$

$$-\frac{\partial p}{\partial x_i} + \mu\frac{\partial^2 u_i}{\partial x_j^2} - C(n\mu UL^2)\frac{\partial}{\partial x_j}\int \mathrm{d}\boldsymbol{p}\, \Omega\left(p_i p_j - \frac{1}{3}\delta_{ij}\right) = n\frac{\partial}{\partial x_j}\int \mathrm{d}\boldsymbol{p}\ \Omega\int_{-L/2}^{L/2} s\,\mathrm{d}s\,\frac{1}{2}(f_i'(s;\boldsymbol{x},\boldsymbol{p})p_j + p_i f_j'(s;\boldsymbol{x},\boldsymbol{p})), \tag{2.17}$$

$$\frac{\partial \Omega}{\partial t} + (Up_i + u_i)\frac{\partial \Omega}{\partial x_i} + \frac{\partial}{\partial p_i}(\dot{p}_i\Omega) - D_r\nabla_p^2\,\Omega + \frac{1}{\tau}\left(\Omega - \int K(\boldsymbol{p}|\boldsymbol{p}')\Omega(\boldsymbol{x},\boldsymbol{p}')\,\mathrm{d}\boldsymbol{p}'\right) = 0, \tag{2.18}$$

where we have now dropped the reference to the mean-field approximation via the superscript 'm', the mean-field force density being denoted by $\boldsymbol{f}'$.

In the homogeneous base state, an isotropic orientation distribution leads to a modified pressure field, but no bulk fluid motion. In other words, $\boldsymbol{u}^{(0)}(\boldsymbol{x},t) = \boldsymbol{0}$, $p^{(0)}(\boldsymbol{x},t) = \mathscr{P}_0$, $\Omega^{(0)} = (4\pi)^{-1}$ is an exact solution of (2.16)–(2.18), $\mathscr{P}_0$ being an arbitrary constant. We now assume small perturbations about this base state given by $\boldsymbol{u} = \boldsymbol{u}'(\boldsymbol{x},t)$, $p = \mathscr{P}_0 + p'(\boldsymbol{x},t)$, and $\Omega = 1/4\pi + \Omega'(\boldsymbol{x},\boldsymbol{p},t)$; the corresponding perturbation in the number density field is given by $n\int\Omega'(\boldsymbol{x},\boldsymbol{p},t)\,\mathrm{d}\boldsymbol{p}$. This leads to the following equations, at linear order, governing the stability of the system to perturbations in the velocity and orientation fields:

$$\frac{\partial u_i'}{\partial x_i} = 0, \tag{2.19}$$

$$-\frac{\partial p'}{\partial x_i} + \mu\frac{\partial^2 u_i'}{\partial x_j^2} - C(n\mu UL^2)\frac{\partial}{\partial x_j}\int \mathrm{d}\boldsymbol{p}\,\Omega'\left(p_i p_j - \frac{1}{3}\delta_{ij}\right) = \frac{n}{4\pi}\frac{\partial}{\partial x_j}\int \mathrm{d}\boldsymbol{p}\int_{-L/2}^{L/2} s\,\mathrm{d}s\,\frac{1}{2}(f_i' p_j + p_i f_j'), \tag{2.20}$$

$$\frac{\partial \Omega'}{\partial t} + Up_i\frac{\partial \Omega'}{\partial x_i} - D_r\nabla_p^2\,\Omega' + \frac{1}{\tau}\left(\Omega' - \int K(\boldsymbol{p}|\boldsymbol{p}')\Omega'(\boldsymbol{x},\boldsymbol{p}',t)\,\mathrm{d}\boldsymbol{p}'\right) = -\frac{1}{4\pi}\frac{\partial \dot{p}_i}{\partial p_i}. \tag{2.21}$$

We note that the convection of the weak orientation anisotropy, Ω', by the perturbation flow field $\boldsymbol{u}'$ has been neglected to linear order. For the same reason, the orientation distribution is assumed to be isotropic when evaluating the passive component of the bacterial stress, since the force density $\boldsymbol{f}'$, unlike the intrinsic force dipole, arises on account of the imposed velocity perturbation; thus, the anisotropy in orientation probability due to the imposed flow only generates a smaller correction at a quadratic order in this case. The stability analysis in the next section is based on (2.19)–(2.21), and is first carried out for a dilute suspension of smooth swimmers ($\tau \to \infty$), in which case the physical interpretation and the form of the neutral curve is the simplest; the analysis for the general case follows thereafter.

In § 3, we argue that a bacterial suspension is most susceptible to long-wavelength disturbances, which are therefore the modes relevant in the determination of the neutral stability curve. Anticipating the dominance of long-wavelength modes, one may approximate the fluid velocity disturbance on length scales of $O(L)$ by a linear shearing flow. Assuming the bacterium to rotate as an axisymmetric body of aspect

ratio r in response to this ambient linear flow, one may write

$$\dot{p}_i = \omega'_{ij} p_j + \mathscr{F}(r)[e'_{ij} p_j - p_i(e'_{jk} p_j p_k)], \tag{2.22}$$

where $\omega'_{ij} = (1/2)(\partial u'_i/\partial x_j - \partial u'_j/\partial x_i)$ and $e'_{ij} = (1/2)(\partial u'_i/\partial x_j + \partial u'_j/\partial x_i)$ are the vorticity and rate of strain tensors associated with the imposed disturbance flow $\boldsymbol{u}'$, and $\mathscr{F}(r)$ is a dimensionless function of the aspect ratio; for a spheroid $\mathscr{F}(r) = (r^2-1)/(r^2+1)$ (see Kim & Karrila 1991) and, in addition, $\mathscr{F}(r)$ approaches unity in the limit of a slender body of an arbitrary cross-section. The second term in brackets in (2.22) acts to preserve the length (head and tail) of the reorienting bacterium. For *E. Coli*, the largest transverse dimension is the diameter of its head which is between 1 and 2 microns, while the combined length of the cell and the flagellar bundle is about 10 microns, leading to an aspect ratio of about 6; thus, $\mathscr{F}(r) \approx 1$ for *E. Coli*.

In the limit of long wavelengths, one may also obtain an expression for the force density, $\boldsymbol{f}'$, as a function of the shape of the bacterium, from the known response of a passive particle of the same shape to an ambient linear flow. For instance, for a spherical bacterium, the symmetric first moment of the force density is just the stresslet associated with a rigid spherical particle; thus, $1/4\pi \int \mathrm{d}\boldsymbol{p} \int_{-L/2}^{L/2} s\,\mathrm{d}s\,(1/2)(f'_i p_j + p_i f'_j) = -(5\pi/6)\,\mu L^3 e'_{ij}$ with L now being the bacterium diameter (see Kim & Karrila 1991). On the other hand, in the limit of large aspect ratios, the linear force density is known from slender-body theory and has only an axial component, being given by $f'_i = -(2\pi\mu s/(\ln r)) p_i(e'_{kl} p_k p_l)$ to leading (logarithmic) order in the aspect ratio (see Batchelor 1970); thus, $1/4\pi \int \mathrm{d}\boldsymbol{p} \int_{-L/2}^{L/2} s\,\mathrm{d}s\,(1/2)(f'_i p_j + p_i f'_j) = -(\pi\mu L^3/45(\ln r))\,e'_{ij}$. For an arbitrary aspect ratio spheroid, a closed-form expression for the integral of the linear force density, although cumbersome, may still be obtained (see Kim & Karrila 1991). In all these cases, we have assumed the bacterium to behave as a rigid inextensible particle. In general, for an axisymmetric bacterium, one may still write $1/4\pi \int \mathrm{d}\boldsymbol{p} \int_{-L/2}^{L/2} s\,\mathrm{d}s\,(1/2)(f'_i p_j + p_i f'_j) = -\mathscr{G}(r)\,\mu L^3 e'_{ij}$, where $\mathscr{G}(r)\,(>0)$ is a function of the aspect ratio, and may also account for a possible compliance or slip at the surface of the bacterium. In the absence of the active stress component, the quantity $(1/2)\,(nL^3)\mathscr{G}(r)$ represents the dimensionless enhancement in the (instantaneous) viscosity of a suspension with an isotropic distribution of axisymmetric particles of aspect ratio r. It is worth noting that for a suspension of passive anisotropic particles, an additional contribution to the viscosity arises on account of Brownian motion; this entropic contribution is again $O(nL^3)$ in the dilute limit, and is due to Brownian torques acting to randomize particle orientations (see Hinch & Leal 1972). A bacterial suspension, however, is fundamentally different in that a swimming (neutrally buoyant) bacterium does not exert any net torque on the fluid. Thus, similar contributions to the suspension viscosity due to the randomizing influences of tumbling and rotary diffusion must stem from moments of the relevant force distributions higher than the first. This is likely to make such contributions numerically small, and we therefore assume the enhancement in viscosity of the bacterial suspension, in the absence of the active stress component, to be entirely on account of hydrodynamic forces.

Since the system under consideration is unbounded and quiescent in its base state, the effect of an arbitrary disturbance may be completely characterized by the response of the system to three-dimensional Fourier modes. The latter response may be obtained by Fourier transforming (2.19)–(2.21). Further, using (2.22) in (2.21), the aforementioned expression for the passive component of the stress induced by the imposed perturbation, and the Fourier transformed equation of continuity, $\hat{u}'_i k_i = 0$,

one obtains

$$-4\pi^2 k^2 \mu \left[1 + \frac{(nL^3)\mathscr{G}(r)}{2}\right] \hat{u}'_i + 2\pi \mathrm{i} C(n\mu U L^2) k_l \int \mathrm{d}\boldsymbol{p}\, \hat{\Omega}' \left(p_l p_j - \frac{1}{3}\delta_{lj}\right)(\delta_{ij} - \hat{k}_i \hat{k}_j) = 0, \tag{2.23}$$

$$\frac{\partial \hat{\Omega}'}{\partial t} - (2\pi \mathrm{i} U)(k_l p_l)\hat{\Omega}' - D_r \nabla_{\boldsymbol{p}}^2 \hat{\Omega}' + \frac{1}{\tau}\left(\hat{\Omega}' - \int K(\boldsymbol{p}|\boldsymbol{p}')\hat{\Omega}'(\boldsymbol{k}, \boldsymbol{p}')\,\mathrm{d}\boldsymbol{p}'\right) = -\frac{3\mathrm{i}}{2}\mathscr{F}(r)(k_i \hat{u}'_j) p_i p_j, \tag{2.24}$$

where $\hat{\boldsymbol{k}} = \boldsymbol{k}/k$ is the unit vector in Fourier space and $(\delta_{ij} - \hat{k}_i \hat{k}_j)$ is a projection operator that serves to eliminate the pressure from the equations of motion. In (2.23) and (2.24), $\hat{\boldsymbol{u}}'(\boldsymbol{k}, t)$ and $\hat{\Omega}'(\boldsymbol{k}, \boldsymbol{p}, t)$ represent the time-dependent Fourier amplitudes of perturbations in the velocity and orientation fields, and we have combined the passive component of the bacterial stress and the stress in the solvent medium into a combined viscous stress with an effective viscosity of $\mu[1 + n\mathscr{G}(r)/2]$; as indicated above, the increased viscosity reflects the stabilizing nature of the passive stress component. The Fourier transform itself is defined as $\hat{g}(\boldsymbol{k}) = \int \mathrm{e}^{2\pi \mathrm{i} \boldsymbol{k}\cdot\boldsymbol{x}} g(\boldsymbol{x})\,\mathrm{d}\boldsymbol{x}$.

We note from the forcing function on the right-hand side of (2.24) that the tensor $p_i p_j$ being symmetric, it is only the symmetric (extensional) part of the velocity gradient, $(k_i \hat{u}'_j + k_j \hat{u}'_i)$, that drives an anisotropy in orientation space. Now, the shearing flow associated with any Fourier mode may be decomposed locally into an extensional and a rotational component, and at linear order, one may superpose the separate effects related to extension and rotation to obtain the net anisotropy in orientation probability. It is then easily seen that the rotational component of the velocity field merely acts to rigidly rotate the isotropic base-state orientation distribution, and it is only the extensional component that generates a peak in orientation along the extensional axis, and thence, an anisotropy. Further, as is evident from (2.22), the function $\mathscr{F}(r)$ is a measure of the relative roles of extension and vorticity in determining the angular velocity of a bacterium. The effect of extension is maximum in the limit of slender bacteria when $\mathscr{F}(r) \approx 1$, and the bacterium rotates as a fluid line element; on the other hand, $\mathscr{F}(r) \to 0$ in the limit $r \to 1$, so that spherical bacteria only respond to the ambient vorticity. Since it is the extensional part of the disturbance flow $\boldsymbol{u}'$ that leads to an anisotropy in orientation, one expects the destabilizing effects of the bacterial stress to be the strongest for slender bacteria. The stability criterion derived in the next section is consistent with this expectation, and the threshold concentration for instability diverges in the limit of spherical bacteria.

3. Stability analysis: calculation of the neutral curve

3.1. *Scaling analysis*

As explained in § 1, the instability of a dilute bacterial suspension is driven by the mutual reinforcement of perturbations in the velocity and orientation fields. Let us examine the anisotropy in the swimming (active) stress induced by an imposed disturbance velocity wave of amplitude u' and wavelength k^{-1}; this anisotropic stress is represented by the last term on the left-hand side in (2.20), and is $O(n\mu U L^2 \Omega')$. The scaling estimate may be understood as the product of the density of force dipoles $(n\mu U L^2)$ times the anisotropy in orientation (Ω'). The rate of accumulation of the destabilizing anisotropy is given by the dilatation in orientation space, that is, $\partial \Omega'/\partial t \propto (\nabla_{\boldsymbol{p}} \cdot \dot{\boldsymbol{p}})$ in (2.21), where the rate of change of orientation due to

the imposed velocity disturbance $\dot{\boldsymbol{p}}$ scales with the velocity gradient ku'. Thus, the total accumulated anisotropy in orientation space (Ω') is the product of the rate of accumulation and an appropriate correlation time, which is a measure of the duration of this accumulation. We denote the latter as t_{corr}, so that $\Omega' \sim O(ku't_{corr})$. The motion of the suspension is driven by the divergence of the resulting anisotropic swimming stress, and is therefore $O(n\mu UL^2k\,\Omega')$. Using the above estimate for Ω', the divergence of the destabilizing swimming stress is $O(n\mu UL^2k^2u't_{corr})$. On the other hand, the stabilizing factor is the viscous response of the Newtonian suspending fluid; the divergence of this viscous stress is $O(\mu[1+(nL^3)\mathscr{G}/2]k^2u')$, and therefore, again $O(k^2)$. Clearly, one expects the destabilizing bacterial stress to become dominant once t_{corr} exceeds a wavelength-independent threshold. Equating the scaling estimates for the swimming and viscous stresses, one obtains that the necessary condition for instability is $t_{corr} > O\{(nUL^2)^{-1}[1+(nL^3)\mathscr{G}/2]\}$. This critical correlation time may be reformulated as a threshold concentration for instability; one obtains

$$(nL^3)_{crit} = (L/Ut_{corr}) \Big/ \left[1 - \frac{L}{Ut_{corr}}\frac{\mathscr{G}(r)}{2}\right].$$

Now we use the above scaling estimates to analyse the instability for various cases. To begin with we consider the limit $D_r \to 0, \tau \to \infty$, when there exists no intrinsic mechanism by which the orientation of an isolated swimming bacterium may decorrelate. For this case, the only limiting factor is the wavelength of the imposed disturbance which is also the distance over which the velocity gradient ku' remains correlated. For instance, if $k > O\{nL^2/[1+(nL^3)\mathscr{G}/2]\}$, the bacteria swims into a region where the velocity gradient has a different sign before accumulating the required orientation anisotropy, and, therefore, the destabilizing swimming stress remains smaller than the critical threshold value. On the other hand, for sufficiently long wavelengths ($k < O\{(nL^2)/[1+(nL^3)\mathscr{G}/2]\}$), the orientation anisotropy continues to accumulate until a time of $O\{(nUL^2)^{-1}[1+(nL^3)\mathscr{G}/2]\}$ when the destabilizing swimming stress overcomes the stabilizing effects of fluid viscosity, and the suspension becomes unstable. This leads us to the conclusion that a suspension of smooth swimmers (pushers), in the limit $D_r \to 0$, is always unstable to sufficiently long-wavelength disturbances at any non-zero bacterial concentration. The neutral curve is trivially given by $(nL^3)_{crit} = 0$ for this limit since $t_{corr} \to \infty$. Of course, this trivial estimate results from the neglect of correlations arising from hydrodynamic interactions. Pairwise interactions lead to a decorrelation in orientation in general, and as will be seen in § 4; pairwise interactions between slender bacteria in particular may be modelled by a hydrodynamic rotary diffusivity (D_r^h), which is, however, sufficiently small, and a suspension of weakly interacting smooth swimmers remains unconditionally unstable.

Next we consider smooth swimmers – $\tau \to \infty$, D_r finite. The orientation bias in this case accumulates only for a time of $O(D_r^{-1})$, and the resulting anisotropy in the orientation distribution, again given by the product of the rate of accumulation (ku') and the correlation time (D_r^{-1}), is $O(ku'/D_r)$. The corresponding swimming stress is now $O\{(n\mu UL^2)(ku'/D_r)\}$. Since, a Newtonian behaviour would lead to the stress of $O(\mu ku')$, we note that the response of a suspension of smooth swimmers to an imposed long-wavelength disturbance is Newtonian, and the swimming viscosity μ_s is $O(\mu nUL^2/D_r)$. Further, on account of the destabilizing nature of the swimming stress (for pushers; $C > 0$), the viscosity μ_s must be negative. In the limit of rapid rotary diffusion $\mu[1+(nL^3)\mathscr{G}/2] \gg \mu_s$, and stability results. However, the suspension of smooth swimmers does become unstable when

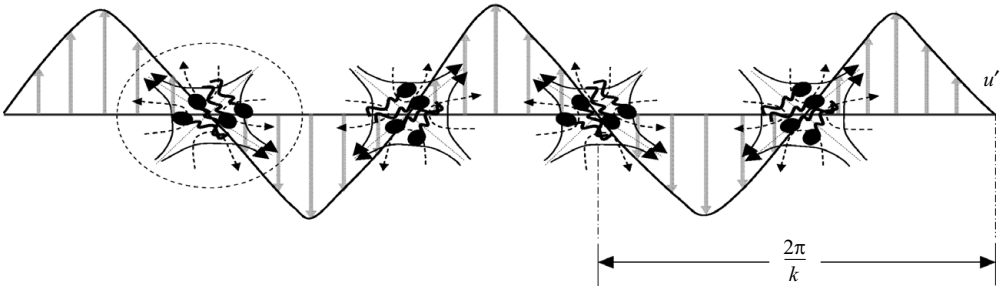

FIGURE 3. The physical mechanism of mutual reinforcement of the velocity and orientation perturbation fields. As the Fourier (velocity) mode grows in amplitude, the orientation distribution in the vicinity of the nodes of the velocity wave becomes increasingly peaked along the local extensional axis; this anisotropy in turn reinforces the velocity perturbation. Note that the local picture as indicated by the dashed circle is identical to the alignment-induced enhancement shown in figure 2.

$\mu_s > \gamma_1\mu[1 + (nL^3)\mathscr{G}/2]$, where γ_1 is a constant, and a function of bacterium shape; the analysis given below determines the value of γ_1 for a bacterium of aspect ratio r. One expects the neutral stability curve for a suspension of smooth swimmers to be of the form $\mu_s/\mu = nUL^2/D_r = \gamma_1[1 + (nL^3)\mathscr{G}/2]$; in other words, the critical concentration $((nL^3)_{crit})$ for instability in a suspension of smooth swimmers must be of the form $\gamma_1(D_rL/U)/[1 - (\gamma_1\mathscr{G}/2)(D_rL/U)]$. Thus, there exists a critical value of the rotary diffusivity $(D_r^{crit} = (2/(\gamma_1\mathscr{G}))(U/L)$ at which the threshold concentration diverges. For D_r larger than this critical value, the destabilizing swimming stress associated with the intrinsic force dipole remains subdominant, and the response of the bacterial suspension is similar to that of a suspension of passive particles. This transition in behaviour is discussed in more detail later when we analyse the general scenario involving decorrelation on account of both rotary diffusion and tumbling. The above condition may also be interpreted as defining the minimum speed of a smooth swimmer $U_{crit} = (D_rL)(\gamma_1\mathscr{G}/2)$ required for instability in a bacterial suspension.

We note that in either of the aforementioned cases, the bacterium needs to swim a distance of $O\{(nL^2)^{-1}[1 + (nL^3)\mathscr{G}/2]\}$ in a time of $O\{(nUL^2)^{-1}[1 + (nL^3)\mathscr{G}/2]\}$ before it accumulates a destabilizing swimming stress of the required magnitude. In the limit $k \to 0$, this distance becomes negligibly small compared to the disturbance wavelength, and one may therefore neglect the translation of the bacterium in (2.24) in the limit of long-wavelength disturbances. The dominant unstable modes thus arise due to the anisotropic stress created by an essentially stationary bacterium orienting in response to an imposed velocity perturbation. The rheological response of the bacterial suspension that results from this anisotropy is, on the scale of $O(k^{-1})$, both local and linear, and thence Newtonian, as indicated by the above scaling arguments. The coupling between the destabilizing velocity and orientation perturbation fields is illustrated in figure 3 from which it should also be evident that the long-wavelength instability will be stationary rather than oscillatory in character. Thus, the principle of exchange of stabilities holds for this case (Chandrasekhar 1961).

3.2. *Neutral curve for smooth swimmers*

Since the long-wavelength disturbances are the most dangerous, these are the modes relevant to the determination of the neutral curve. We now exploit the above

simplifications in the limit $k \to 0$ to first determine the neutral curve for a suspension of smooth swimmers ($\tau \to \infty$) before proceeding to the general case of arbitrary (τD_r). First, taking the limit $\tau \to \infty$ in (2.23) and (2.24), one has the following equations governing the evolution of Fourier modes in a suspension of smooth swimmers:

$$-4\pi^2 k^2 \mu \left[1 + \frac{(nL^3)\mathscr{G}(r)}{2}\right] \hat{u}'_i + 2\pi \mathrm{i} C(n\mu U L^2) k_l \int \mathrm{d}\boldsymbol{p}\, \hat{\Omega}' \times \left(p_l p_j - \frac{1}{3}\delta_{lj}\right)(\delta_{ij} - \hat{k}_i \hat{k}_j) = 0, \quad (3.1)$$

$$\frac{\partial \hat{\Omega}'}{\partial t} - (2\pi \mathrm{i} U)(k_l p_l)\hat{\Omega}' - D_r \nabla_{\boldsymbol{p}}^2 \hat{\Omega}' = -\frac{3\mathrm{i}}{2}\mathscr{F}(r)(k_i \hat{u}'_j) p_i p_j. \quad (3.2)$$

On account of the stationary nature of the unstable long-wavelength modes, one may set $\partial \hat{\Omega}'/\partial t = 0$. Further, neglecting the effect of translation in (3.2) (this term is $O(k)$ in the limit $k \to 0$), one obtains the following simplified system of equations on the neutral stability curve for a suspension of smooth swimmers:

$$-4\pi^2 k^2 \mu \left[1 + \frac{(nL^3)\mathscr{G}(r)}{2}\right] \hat{u}'_i + 2\pi \mathrm{i} C(n\mu U L^2) k_l \int \mathrm{d}\boldsymbol{p}\, \hat{\Omega}' \times \left(p_l p_j - \frac{1}{3}\delta_{lj}\right)(\delta_{ij} - \hat{k}_i \hat{k}_j) = 0, \quad (3.3)$$

$$-D_r \nabla_{\boldsymbol{p}}^2 \hat{\Omega}' = -\frac{3\mathrm{i}}{2}\mathscr{F}(r)(k_i \hat{u}'_j) p_i p_j. \quad (3.4)$$

It is readily seen that the solution of (3.4) must be of the form $\hat{\Omega}' = \mathscr{C}' k_i \hat{u}'_j p_i p_j$; one finds $\mathscr{C}' = -(\mathrm{i}/4D_r)\mathscr{F}(r)$ on substitution. This anisotropy in the orientation distribution is the one expected for a balance of shear and rotary Brownian motion in the limit of weak shear. The perturbation in orientation is thus aligned with the local extensional axis of the flow in accordance with earlier arguments at the end of § 2, and in agreement with the illustration in figure 3. This corresponds, in fact, to a Newtonian viscous response similar to that of a suspension of Brownian rods, except with an opposite sign owing to the difference in direction of the bacterium force dipole; the latter may be seen by substitution into the equations of motion. Indeed, using $\hat{\Omega}' = -(\mathrm{i}/4D_r)\mathscr{F}(r) k_i \hat{u}'_j p_i p_j$ in (3.3), one obtains

$$-4\pi^2 k^2 \mu \left[1 + \frac{(nL^3)\mathscr{G}(r)}{2}\right] \hat{u}'_i - 2\pi \mathrm{i} C(n\mu U L^2) k_l (\delta_{ij} - \hat{k}_i \hat{k}_j) \times \left[\int \mathrm{d}\boldsymbol{p}\, p_l p_j p_m p_n\right] \frac{\mathrm{i}}{4D_r}\mathscr{F}(r) k_m \hat{u}'_n = 0. \quad (3.5)$$

Further, on using the standard result for the integration of a unit normal polyad over the surface of a unit sphere (see Bird, Armstrong & Hassager 1987)

$$\int p_l p_j p_m p_n \,\mathrm{d}\boldsymbol{p} = \frac{4\pi}{15}(\delta_{lj}\delta_{mn} + \delta_{lm}\delta_{jn} + \delta_{ln}\delta_{jm}),$$

and the incompressibility of the fluid velocity field (3.5) simplifies to

$$\left[-4\pi^2 \left[1 + \frac{(nL^3)\mathscr{G}(r)}{2}\right] \mu + \frac{2\pi^2 C}{15}\left(\frac{n\mu U L^2}{D_r}\right)\mathscr{F}(r)\right] k^2 \hat{u}'_i = 0. \quad (3.6)$$

Assuming $C > 0$, as is the case for a pusher, the equation for the neutral stability curve is given by

$$\left(\frac{nUL^2}{D_r}\right) = \frac{30}{C\mathscr{F}(r)}\left[1 + \frac{(nL^3)\mathscr{G}(r)}{2}\right], \quad \Rightarrow (nL^3)_{crit} = \frac{\dfrac{30}{C\mathscr{F}(r)}\left(\dfrac{D_r L}{U}\right)}{\left[1 - \dfrac{15\mathscr{G}(r)}{C\mathscr{F}(r)}\left(\dfrac{D_r L}{U}\right)\right]} \tag{3.7}$$

for a suspension of smooth swimmers. This is consistent with the general form anticipated from earlier scaling arguments for smooth swimmers. In particular, the analysis yields the value of the constant γ_1 appearing in this general form; $\gamma_1 = 30/(C\mathscr{F}(r))$. The critical value of D_r above which the suspension is stable at all concentrations is

$$D_r^{crit} = \frac{\dfrac{C}{\mathscr{F}(r)}}{15\mathscr{G}(r)}\left(\frac{U}{L}\right).$$

From (3.6), it is seen that for rotary diffusivities greater than this critical value, the effective viscosity of the stable bacterial suspension is given by

$$\mu_B = \mu\left[1 + \frac{(nL^3)\mathscr{G}(r)}{2}\left(1 - \frac{C\mathscr{F}(r)}{15\mathscr{G}(r)}\left(\frac{U}{LD_r}\right)\right)\right].$$

The value of C for a given species of bacterium may be readily estimated from the drag exerted on the fluid by its head when swimming.

Following Liao *et al.* (2007), we now estimate C for an *E. Coli*, assuming a constant force density along both the head and tail of the swimming bacterium. Slender body, at leading order, does predict a constant force density in translation; thus, the higher (effective) aspect ratio of the helical tail ensures that the above assumption is more accurate for the tail than it is for the head. The latter may be approximated by a spheroid of aspect ratio 2. With the assumption of a constant force density, and the neglect of any hydrodynamic interaction between the head and tail, one only needs the total drag F_D on the head in order to obtain an estimate for the force density $\boldsymbol{f}$ in (2.3); the helical tail, of course, exerts an equal and opposite propulsive force. From the known expression for the Stokes drag on a spheroid of aspect ratio r_e translating along its axis (see Happel & Brenner 1973), one may write $F_D = M^{-1}\mu U L_H$, L_H being the length of the head. Here, the axial mobility coefficient M is given by

$$M = \frac{1}{8\pi}\left[-\frac{2r_e^2}{(r_e^2-1)} + \frac{(2r_e^3 - r_e)}{(r_e^2-1)^{3/2}}\ln\left\{\frac{r_e + (r_e^2-1)^{1/2}}{r_e - (r_e^2-1)^{1/2}}\right\}\right]. \tag{3.8}$$

Thus, $\boldsymbol{f}(s) = M^{-1}\mu U\boldsymbol{p}$ on the head ($(1/2-\alpha)L < s < L/2$), where $\alpha = L_H/L \approx 0.2$ for an *E. Coli*; further $\boldsymbol{f}(s) = -\alpha/(1-\alpha)M^{-1}\mu U\boldsymbol{p} \approx -0.25M^{-1}\mu U\boldsymbol{p}$ on the tail ($-L/2 < s < (1/2-\alpha)L$). Using (2.3), one obtains

$$\boldsymbol{\sigma}^B = -\frac{n}{2}\int \mathrm{d}\boldsymbol{p}\, \Omega(\boldsymbol{x}, \boldsymbol{p}, t)\left(\boldsymbol{pp} - \frac{1}{3}\boldsymbol{\delta}\right)\left[\int_{(1/2-\alpha)L}^{L/2} M^{-1}\mu U s\,\mathrm{d}s - \int_{-L/2}^{(1/2-\alpha)L}\frac{\alpha}{(1-\alpha)}M^{-1}\mu U s\,\mathrm{d}s\right], \tag{3.9}$$

$$= -\frac{\alpha}{2}M^{-1}(n\mu UL^2)\int \mathrm{d}\boldsymbol{p}\ \Omega(\boldsymbol{x}, \boldsymbol{p}, t)\left(\boldsymbol{pp} - \frac{1}{3}\boldsymbol{\delta}\right). \tag{3.10}$$

On comparison with (2.15), one finds $C \approx (\alpha/2)M^{-1}$. Finally, using $\alpha = 0.2$, and (3.8) with $r_e = 2$, one obtains $C \approx 0.57$ for the case of *E. Coli*. Thus, for the smooth-swimming mutant strain of *E. Coli* (for instance, the strain *RP*9535 used by Wu *et al.* 2006), equation (3.7) for the neutral curve corresponds to the following threshold concentration:

$$(nL^3)^{E.Coli}_{crit} = \frac{52.6(D_r L/U)}{[1 - 2.05(D_r L/U)]}. \tag{3.11}$$

for instability; in (3.11), we have used the limiting values of $\mathscr{F}(r)\,(\approx 1)$ and $\mathscr{G}(r)\,(\approx 2\pi/(45(\ln r)))$ for a slender bacterium.

3.3. *Neutral curve for wild-type tumblers*

Moving on to the general case, where the bacteria execute a run-and-tumble motion (the wild-type *E. Coli* strain), we note that tumbling provides an additional mechanism for limiting the orientational bias accumulated by a swimming bacterium. In the limit of small τ (specifically, $\tau \ll D_r^{-1}$), for instance, an imposed velocity disturbance, even in the limit of long wavelengths, acts to orient a bacterium only until it tumbles, and the anisotropy in the orientation distribution is now $O(ku'\tau)$. The equation for the neutral curve in this limit therefore takes the form $nUL^2\tau = \gamma_2[1 + (nL^3)\mathscr{G}(r)/2]$, where γ_2 is again a function of the bacterium shape, and the correlation parameter (β) characterizing the tumbling events. Similar to the case of rapid rotary diffusion, the anisotropy in the swimming stress, in the limit of small bacterial number densities or high tumbling frequencies, is not enough to overcome the stabilizing contributions arising from the solvent viscosity and the passive stress component. The bacterial suspension is stable for concentrations less than $(L/(U\tau))\gamma_2/[1-(\gamma_2\mathscr{G}/2)(L/(U\tau))]$, and when the tumbling time decreases below a critical value of $(\gamma_2\mathscr{G}/2)(L/U)$, the suspension is unconditionally stable. Interestingly, there does exist an experimental realization of this rapid tumbling limit. Wu *et al.* (2006) measured the translational diffusivity of a mutant strain of *E. Coli* wherein mutation led to the rotation of the flagella in the clockwise direction alone, in turn leading to an incessant tumbling behaviour (for the case of smooth swimmers, the mutation causes the flagellar bundle to rotate only in the counterclockwise direction). Although the translational diffusivity was only measured for a single concentration for these rapid tumblers, the values of the diffusivities at this concentration were nevertheless much lower than those for smooth swimmers or the wild-type strain.

In the general case when tumbling and rotary diffusion occur on comparable time scales, one anticipates a neutral curve of the general form $nUL^2/D_r = \gamma_3 f(\tau D_r; \beta)[1 + (nL^3)\mathscr{G}(r)/2]$, where γ_3 is a function of the aspect ratio for a slender bacterium, and β is the correlation parameter in the transition probability $K(\boldsymbol{p}|\boldsymbol{p}')$ governing a tumbling event. Evidently, for $\tau D_r \to \infty$, or equivalently, in the limit of perfectly correlated tumbles $(\beta \to \infty)$, the general equation for the neutral curve must reduce to the form $(nUL^2/D_r) = (30/C\mathscr{F}(r))[1 + (nL^3)\mathscr{G}(r)/2]$, found earlier for the case of smooth swimmers.

We now proceed to determine the form of the neutral curve when $\tau D_r \sim O(1)$. To begin with, we note that even in the presence of both tumbling and rotary diffusion, a bacterium has to swim the same distance of $O(nL^2)^{-1}[1+(nL^3)\mathscr{G}(r)/2]$, asymptotically small in relation to the wavelength k^{-1} of the imposed velocity disturbance in the limit $k \to 0$, in order to accumulate the necessary orientational bias for instability; in addition, the resulting instability continues to be stationary in character. Therefore, for purposes of determining the neutral stability curve, one may again neglect both $\partial\hat{\Omega}'/\partial t$ and the translation term in (2.24), leading to the following simplified set of

equations:

$$-4\pi^2 k^2 \mu \left[1 + \frac{(nL^3)\mathscr{G}(r)}{2}\right] \hat{u}_i' + (2\pi \mathrm{i} C) k_l \int \mathrm{d}\boldsymbol{p}\ \hat{\Omega}' \left(p_l p_j - \frac{1}{3}\delta_{lj}\right)(\delta_{ij} - \hat{k}_i \hat{k}_j) = 0, \quad (3.12)$$

$$\nabla_p^2 \hat{\Omega}' = \frac{1}{(\tau D_r)} \left(\hat{\Omega}' - \int K(\boldsymbol{p}|\boldsymbol{p}') \hat{\Omega}'(\boldsymbol{k}, \boldsymbol{p}')\, \mathrm{d}\boldsymbol{p}'\right) + \frac{3\mathrm{i}}{2} \left(\frac{nUL^2}{D_r}\right) \mathscr{F}(r)(k_i \hat{u}_j') p_i p_j. \quad (3.13)$$

We have used the scales U and nL^2 for the velocity field and wavenumber, respectively, while continuing to use the same symbols for the resulting dimensionless variables in the interests of notational simplicity. It now becomes convenient to first write down the formal solution of (3.13) in terms of a modified Green's function $G_M(\boldsymbol{p}|\boldsymbol{p}')$ of the orientation Laplacian as

$$\hat{\Omega}' = \frac{1}{(\tau D_r)} \int G_M(\boldsymbol{p}|\boldsymbol{p}') \left[\hat{\Omega}'(\boldsymbol{k}, \boldsymbol{p}') - \int K(\boldsymbol{p}'|\boldsymbol{p}'') \hat{\Omega}'(\boldsymbol{k}, \boldsymbol{p}'')\mathrm{d}\boldsymbol{p}''\right] \mathrm{d}\boldsymbol{p}' + \frac{3\mathrm{i}}{2} \left(\frac{nUL^2}{D_r}\right) \mathscr{F}(r) k_i \hat{u}_j' \int G_M(\boldsymbol{p}|\boldsymbol{p}') p_i' p_j'\, \mathrm{d}\boldsymbol{p}', \quad (3.14)$$

where

$$\nabla_p^2 G_M(\boldsymbol{p}|\boldsymbol{p}') = \delta(\boldsymbol{p} - \boldsymbol{p}') - \frac{1}{4\pi}. \quad (3.15)$$

The need for a modified Green's function arises because the orientational Laplacian has a zero eigenvalue corresponding to a steady isotropic distribution on the unit sphere, and the usual Green's function is therefore not well defined. However, in the present case, conservation of probability in orientation space implies that the forcing function (terms on the right-hand side) in (3.13) has a net zero contribution when integrated over the unit sphere. Physically, one only needs the perturbative response to a redistribution of probability in orientation space rather than to a net addition, and the use of $G_M(\boldsymbol{p}|\boldsymbol{p}')$ is therefore appropriate. The modified Green's function is given by

$$G_M(\boldsymbol{p}|\boldsymbol{p}') = -\frac{1}{4\pi} \sum_{n=1}^{\infty} \frac{(2n+1)}{n(n+1)} P_n(\boldsymbol{p} \cdot \boldsymbol{p}'), \quad (3.16)$$

where $G_M(\boldsymbol{p}|\boldsymbol{p}')$ describes the long-time response to a rearrangement of an initially isotropic distribution of orientational probability into a perfectly aligned one, the direction of alignment being given by $\boldsymbol{p}'$. In (3.16), P_n is the Legendre polynomial of the nth degree, and we note that the summation does not include P_0 as discussed above. In spherical polar coordinates, $\boldsymbol{p} \cdot \boldsymbol{p}' = \cos\theta_1 \cos\theta_2 + \sin\theta_1 \sin\theta_2 \cos\phi$, where θ_1 and θ_2 are, respectively, the polar angles of the points $\boldsymbol{p}$ and $\boldsymbol{p}'$ on the unit sphere, and ϕ the azimuthal angle between them. Further, on use of the well-known addition theorem for Legendre polynomials (for instance, see Gradshteyn & Ryzhik 1965), the above expression reduces to the familiar form of the fundamental solution of the orientational Laplacian given in mathematical texts. Rather surprisingly, one does not need the detailed expression for G_M; indeed, it will be seen that the necessary information may, in fact, be obtained from the form of the neutral curve for smooth swimmers ($\tau \to \infty$) derived earlier (see (3.7)).

With $G_M(\boldsymbol{p}|\boldsymbol{p}')$ known, one may write down the formal solution of (3.14), a Fredholm integral equation of the second kind, as a Neumann series

$$\hat{\Omega}' = \left[1 + \frac{1}{(\tau D_r)}\mathscr{G} + \frac{1}{(\tau D_r)^2}\mathscr{G}^2 + \cdots\right] \frac{3\mathrm{i}}{2}\left(\frac{nUL^2}{D_r}\right) \mathscr{F}(r) k_i \hat{u}'_j \int G_M(\boldsymbol{p}|\boldsymbol{p}') p'_i p'_j \,\mathrm{d}\boldsymbol{p}, \tag{3.17}$$

where the convergence of the above formal series will be demonstrated by explicit summation. In (3.17), the operator $\mathscr{G}$ is defined by

$$\mathscr{G}(.) = \int \left[G_M(\boldsymbol{p}|\boldsymbol{p}') - \left\{\int \mathrm{d}\boldsymbol{p}'' G_M(\boldsymbol{p}|\boldsymbol{p}'') K(\boldsymbol{p}''|\boldsymbol{p}')\right\}\right](.)\mathrm{d}\boldsymbol{p}'. \tag{3.18}$$

In order to evaluate $\hat{\Omega}'$, we will need the following two results proved in appendix B:

$$k_i \hat{u}_j \int K(\boldsymbol{p}|\boldsymbol{p}') p'_i p'_j \mathrm{d}\boldsymbol{p}' = \left[\frac{(3+\beta^2)\sinh\beta - 3\beta\cosh\beta}{\beta^2 \sinh\beta}\right](k_i \hat{u}'_j) p_i p_j, \tag{3.19}$$

$$k_i \hat{u}_j \int G_M(\boldsymbol{p}|\boldsymbol{p}') p'_i p'_j \mathrm{d}\boldsymbol{p}' = \mathscr{C}(k_i \hat{u}'_j) p_i p_j, \tag{3.20}$$

where the constant $\mathscr{C}$ would, in principle, be determined using (3.16) for $G_M(\boldsymbol{p}|\boldsymbol{p}')$. However, it turns out that $\mathscr{C}$ may also be evaluated using neutral curve (3.7) derived earlier for smooth swimmers. Using (3.19) and (3.20), we have

$$k_i \hat{u}'_j \mathscr{G}(p_i p_j) = k_i \hat{u}'_j \left[\mathscr{C} p_i p_j - \frac{(3+\beta^2)\sinh\beta - 3\beta\cosh\beta}{\beta^2\sinh\beta} \times \int \mathrm{d}\boldsymbol{p}' G_M(\boldsymbol{p}|\boldsymbol{p}') p'_i p'_j\right], \tag{3.21}$$

$$= \mathscr{C}\left[1 - \frac{(3+\beta^2)\sinh\beta - 3\beta\cosh\beta}{\beta^2\sinh\beta}\right](k_i \hat{u}'_j) p_i p_j, \tag{3.22}$$

$$= 3\mathscr{C}\frac{(\beta\cosh\beta - \sinh\beta)}{\beta^2\sinh\beta}(k_i \hat{u}'_j) p_i p_j. \tag{3.23}$$

Using (3.23) in (3.17), one obtains

$$\hat{\Omega}' = \left[1 + \frac{3\mathscr{C}}{(\tau D_r)}\frac{(\beta\cosh\beta - \sinh\beta)}{\beta^2\sinh\beta} + \frac{9\mathscr{C}^2}{(\tau D_r)^2}\frac{(\beta\cosh\beta - \sinh\beta)^2}{\beta^4\sinh^2\beta} + \cdots\right] \times \frac{3\mathrm{i}\mathscr{C}}{2}\mathscr{F}(r)\left(\frac{nUL^2}{D_r}\right) k_i \hat{u}'_j p_i p_j, \tag{3.24}$$

$$= \frac{1}{\left[1 - \dfrac{3\mathscr{C}}{(\tau D_r)}\dfrac{(\beta\cosh\beta - \sinh\beta)}{\beta^2\sinh\beta}\right]} \frac{3\mathrm{i}\mathscr{C}}{2}\mathscr{F}(r)\left(\frac{nUL^2}{D_r}\right) k_i \hat{u}'_j p_i p_j. \tag{3.25}$$

Now, using (3.25) for $\hat{\Omega}'$ in equations of motion (3.12), one has the following relation in terms of the Fourier amplitude of the velocity field alone:

$$\hat{u}_i' = -\hat{u}_n' \left[\frac{3C\mathscr{C}}{4\pi k^2} \mathscr{F}(r) \frac{k_l k_m (\delta_{ij} - \hat{k}_i \hat{k}_j)}{\left[1 - \frac{3\mathscr{C}}{(\tau D_r)} \frac{(\beta \cosh \beta - \sinh \beta)}{\beta^2 \sinh \beta}\right] \left[1 + \frac{(nL^3)\mathscr{G}(r)}{2}\right]} \right] \times \left(\frac{nUL^2}{D_r}\right) \int p_l p_j p_m p_n \, \mathrm{d}\boldsymbol{p}. \quad (3.26)$$

The above relation is of the general form $\hat{u}_i' = -\mathscr{T}_{in} \hat{u}_n'$. Since $\hat{u}_i' k_i = 0$, $\mathscr{T}_{in}$ must be of the general form $-\delta_{in} + q\hat{k}_i \hat{k}_n$, q being an arbitrary constant. However, $\mathscr{T}_{in}$ as defined by (3.26) is proportional to $(\delta_{ij} - \hat{k}_i \hat{k}_j)$, and is therefore orthogonal to $\hat{k}_i$. This additional orthogonality condition implies $q = 1$, so that

$$\left[\frac{3C\mathscr{C}}{4\pi k^2} \mathscr{F}(r) \frac{k_l k_m (\delta_{ij} - \hat{k}_i \hat{k}_j)}{\left[1 - \frac{3\mathscr{C}}{(\tau D_r)} \frac{(\beta \cosh \beta - \sinh \beta)}{\beta^2 \sinh \beta}\right] \left[1 + \frac{(nL^3)\mathscr{G}(r)}{2}\right]} \right] \times \left(\frac{nUL^2}{D_r}\right) \int p_l p_j p_m p_n \, \mathrm{d}\boldsymbol{p} = -\delta_{in} + \hat{k}_i \hat{k}_n, \quad (3.27)$$

Using $i = n$, and the known result quoted above for the orientational integral, the equation for the neutral stability curve as a function of (τD_r) and (nUL^2/D_r) finally takes the form

$$\left(\frac{nUL^2}{D_r}\right) = -\frac{5}{C\mathscr{C}\mathscr{F}(r)} \left[1 - \frac{3\mathscr{C}}{(\tau D_r)} \frac{(\beta \cosh \beta - \sinh \beta)}{\beta^2 \sinh \beta}\right] \left[1 + \frac{(nL^3)\mathscr{G}(r)}{2}\right]. \quad (3.28)$$

The constant $\mathscr{C}$ may now be determined by comparing (3.28) with its appropriate limiting form (3.7) for $\tau \to \infty$; this gives $\mathscr{C} = -1/6$, and thus, the neutral stability curve for the general case is

$$\left(\frac{nUL^2}{D_r}\right) = \frac{30}{C\mathscr{F}(r)} \left[1 + \frac{1}{2(\tau D_r)} \frac{(\beta \cosh \beta - \sinh \beta)}{\beta^2 \sinh \beta}\right] \left[1 + \frac{(nL^3)\mathscr{G}(r)}{2}\right]. \quad (3.29)$$

As before, criterion (3.29) is more conveniently formulated in terms of a critical non-dimensional bacterial concentration. To this end, (3.29) may be rewritten as

$$(nL^3)_{crit} = \frac{\frac{30}{C\mathscr{F}(r)} \left(\frac{D_r L}{U}\right) \left[1 + \frac{1}{2\tau D_r} \frac{(\beta \cosh \beta - \sinh \beta)}{\beta^2 \sinh \beta}\right]}{\left\{1 - \frac{15\mathscr{G}(r)}{C\mathscr{F}(r)} \left(\frac{D_r L}{U}\right) \left[1 + \frac{1}{2\tau D_r} \frac{(\beta \cosh \beta - \sinh \beta)}{\beta^2 \sinh \beta}\right]\right\}}. \quad (3.30)$$

As was the case for smooth swimmers, the critical concentration given by (3.30) diverges when the orientation decorrelation becomes sufficiently rapid. This divergence occurs when

$$\frac{15\mathscr{G}(r)}{C\mathscr{F}(r)} \left(\frac{D_r L}{U}\right) \left[1 + \frac{1}{2\tau D_r} \frac{(\beta \cosh \beta - \sinh \beta)}{\beta^2 \sinh \beta}\right] \to 1,$$

where the factor,

$$\frac{15\mathscr{G}(r)}{C\mathscr{F}(r)} \left(\frac{D_r L}{U}\right) \left[1 + \frac{1}{2\tau D_r} \frac{(\beta \cosh \beta - \sinh \beta)}{\beta^2 \sinh \beta}\right],$$

is a measure of the rate of decorrelation in the presence of both diffusion and tumbling. This is easily seen by noting that two decorrelation processes (rotary diffusion and tumbling) occur in parallel and the overall correlation time may then be obtained from a parallel combination of the individual correlation times now regarded as resistances. The overall rate of decorrelation is given by the reciprocal of this correlation time. In light of this, the aforementioned criterion for the divergence of the critical concentration is more conveniently expressed in the terms of a threshold for the correlation time viz $\bar{t}_{corr} \to 1$, where $\bar{t}_{corr}$, the correlation time in units of $(\mathscr{G}(r)/2C\mathscr{F}(r))(L/U)$, is given by $1/\bar{t}_{corr} = 1/\bar{t}_{diff} + 1/\bar{t}_{tumble}$, with $\bar{t}_{diff} = (C/30)D_r^{-1}$ and $\bar{t}_{tumble} = (\beta\cosh\beta - \sinh\beta)\tau/(15\beta^2\sinh\beta)$ (see (3.11) and (3.31)). The reason for the choice of scale for $\bar{t}_{corr}$ may be traced to the scaling arguments presented at the beginning of this section, where we noted that the destabilizing orientation stress needs to accumulate over a time of $O\{(nUL^2)^{-1}[1 + (nL^3)\mathscr{G}(r)/2]\}$ for instability to occur; thus, the minimum correlation time required for instability is $O(L\mathscr{G}(r)/2U)$ in the limit $nL^3 \to \infty$, which is therefore a natural scale for $\bar{t}_{corr}$. The additional factor $1/(C\mathscr{F}(r))$ accounts for the effects of the dimensionless dipole strength C and the bacterium aspect ratio. Clearly, when $\bar{t}_{corr} < 1$, the orientation decorrelation on account of rotary diffusion and tumbling occurs in a time shorter than the minimum time scale needed for instability. Therefore, the bacterial suspension, in response to an imposed long-wavelength perturbation, behaves in a manner similar to a suspension of passive particles with an effective viscosity given by

$$\mu_{eff} = \mu\left[1 + \frac{(nL^3)\mathscr{G}(r)}{2}\left(1 - \frac{\dfrac{C\mathscr{F}(r)}{15\mathscr{G}(r)}\left(\dfrac{U}{D_rL}\right)}{\left[1 + \dfrac{1}{2\tau D_r}\dfrac{(\beta\cosh\beta - \sinh\beta)}{\beta^2\sinh\beta}\right]}\right)\right].$$

As noted earlier in the context of smooth swimmers, the divergence of the threshold concentration may also be interpreted in terms of a critical swimming speed for instability in a suspension of wild-type tumblers. Thus, below a swimming speed of

$$U_{crit} = (D_rL)\frac{15\mathscr{G}(r)}{C\mathscr{F}(r)}\left[1 + \frac{1}{2\tau D_r}\frac{(\beta\cosh\beta - \sinh\beta)}{\beta^2\sinh\beta}\right],$$

the magnitude of the intrinsic force dipole and the resulting swimming stress remain smaller than the stabilizing viscous stress for all concentrations.

In the limit $D_r \to 0$ with τ fixed, the expression for the threshold concentration takes the form

$$\lim_{D_r\to 0}(nL^3)_{crit} = \frac{\dfrac{15}{C\mathscr{F}(r)}\left(\dfrac{L}{U\tau}\right)\dfrac{(\beta\cosh\beta - \sinh\beta)}{\beta^2\sinh\beta}}{1 - \dfrac{15\mathscr{G}(r)}{2C\mathscr{F}(r)}\left(\dfrac{L}{U\tau}\right)\dfrac{(\beta\cosh\beta - \sinh\beta)}{\beta^2\sinh\beta}}, \tag{3.31}$$

again consistent with that anticipated above in the limit of small τ, viz $nUL^2\tau = \gamma_2[1 + nL^3\mathscr{G}(r)/2]$ with

$$\gamma_2 = \frac{15}{C\mathscr{F}(r)}\left(\frac{L}{U\tau}\right)\frac{(\beta\cosh\beta - \sinh\beta)}{\beta^2\sinh\beta}.$$

Further, for uncorrelated tumbling, one obtains

$$\lim_{D_r\to 0,\beta\to 0}(nL^3)_{crit} = \frac{\dfrac{5}{C\mathscr{F}(r)}\left(\dfrac{L}{U\tau}\right)}{1-\dfrac{5\mathscr{G}(r)}{2C\mathscr{F}(r)}\left(\dfrac{L}{U\tau}\right)}, \tag{3.32}$$

where we have used that $\lim_{\beta\to 0}(\beta\cosh\beta-\sinh\beta)/(\beta^2\sinh\beta)=1/3$. With $\beta\approx 1$, as is the case for *E. Coli*, this function of β is about 0.31. Thus, a moderate bias towards tumbles of less than 90° changes the correlation function only by about 6 %, and at least for *E. Coli*, one expects the random-tumble approximation to yield an accurate estimate for the threshold concentration. Thus, letting $\beta\to 0$ in (3.30), one obtains

$$(nL^3)_{crit} = \frac{\dfrac{30}{C\mathscr{F}(r)}\left(\dfrac{D_rL}{U}\right)\left[1+\dfrac{1}{6\tau D_r}\right]}{\left\{1-\dfrac{15\mathscr{G}(r)}{C\mathscr{F}(r)}\left(\dfrac{D_rL}{U}\right)\left[1+\dfrac{1}{6\tau D_r}\right]\right\}}, \tag{3.33}$$

for the threshold concentration in the limit of perfectly random tumbles. Finally, we note that the critical concentration given by (3.30) approaches zero in the limit $D_r\to 0, \tau\to\infty$ (or alternatively, $D_r\to 0$ with τD_r fixed), implying that a suspension of 'straight swimmers' is always unstable.

It needs to be emphasized that the instability analysed here pertains to fluctuations in the orientation and velocity fields. Rather remarkably, it is seen from (3.25) that the perturbation in the number density field, given by $n\int\hat{\Omega}'\mathrm{d}\boldsymbol{p}$, is identically zero at the linear order of approximation. Thus, at least for the dominant unstable modes, the concentration field in the unstable bacterial suspension still remains spatially homogeneous. This latter fact remains true even outside the long-wavelength limit, and is merely a consequence of incompressibility and fore-aft symmetry ($\boldsymbol{p}\leftrightarrow-\boldsymbol{p}$). With these constraints, there exists no scalar combination of $\boldsymbol{u}$ and $\boldsymbol{k}$ that would lead to a non-trivial amplitude for the number density wave, and an initial condition that respects the $\boldsymbol{p}\leftrightarrow-\boldsymbol{p}$ symmetry cannot therefore lead to an inhomogeneous number density field. This may also be seen from the governing equation for Ω; an integration of (2.5) over orientation space yields

$$\frac{\partial}{\partial t}(n\textstyle\int\Omega\,\mathrm{d}\boldsymbol{p})+\boldsymbol{u}\cdot\nabla_{\boldsymbol{x}}\left(n\int\Omega\,\mathrm{d}\boldsymbol{p}\right)+\nabla_{\boldsymbol{x}}\cdot\left(\int U\boldsymbol{p}\,\Omega\,\mathrm{d}\boldsymbol{p}\right)=0. \tag{3.34}$$

The last term in (3.34) vanishes when $\Omega(\boldsymbol{p})=\Omega(-\boldsymbol{p})$, and in this case, the number density perturbation evolves only on account of convection by an incompressible fluid velocity field. Clearly, an initially homogeneous number density field will then continue to remain homogeneous. Physically, for every bacterium that swims into a given region, acting to enhance the local number density, there corresponds another bacterium with an exactly opposing orientation, exerting the same destabilizing influence on the velocity and orientation fields, but acting instead to reduce the number density in the same region by swimming out of it. This physical argument evidently does not rely on the perturbations being infinitesimally small. It therefore appears that even in presence of interactions, and in the nonlinear regime, the fundamental difference between the nature of the number density fluctuations and the velocity and orientation field fluctuations, arising at the linear approximation, may persist, for instance, as a difference in the relevant correlation times. The generation of number density fluctuations requires a breaking of the $\boldsymbol{p}\leftrightarrow-\boldsymbol{p}$ symmetry and

dynamics (not considered here) that would amplify the resulting asymmetry. Such an amplification naturally arises on account of directed swimming in polar active nematics (Simha & Ramaswamy 2002), but could also arise from fluctuations due to a discrete number of bacteria as is the case in simulations (Saintillan & Shelley 2007).

4. Effect of hydrodynamic interactions on the stability of a dilute bacterial suspension

Herein, we focus on the effects of correlations induced by hydrodynamic interactions in a dilute suspension of otherwise straight swimmers. Experiments with bacterial suspensions are not easy, since, amongst other difficulties, the bacterial swimming characteristics remain sensitive to the method of culturing, nutrient concentration, etc., making reproducibility and comparison with theoretical predictions difficult. Simulations of active swimmers therefore offer a valuable tool to gain insight into the dynamics of this complex system. All simulation efforts thus far have been restricted to the case of straight swimmers ($D_r = 0, \tau \to \infty$), wherein the collective dynamics is entirely driven by hydrodynamic interactions (for instance, see Hernandez-Ortiz *et al.* 2005; Saintillan & Shelley 2007). From the point of view of the stability analysis detailed in the previous section, there exists no intrinsic decorrelation mechanism in these simulations, and the orientation of a swimmer decorrelates only due to interactions. With this in mind, we now examine a dilute bacterial suspension in the limit $\tau \to \infty$, and for the case where a rotary diffusion arises from pair-hydrodynamic interactions rather than any imperfections inherent in the swimming mechanism; in order to emphasize the hydrodynamic origin of the orientation decorrelation process, we will denote the resulting hydrodynamic rotary diffusivity by D_r^h in the analysis that follows. The objective then is to derive an expression for D_r^h, and thereby, predict the threshold concentration for instability in a suspension of weakly interacting smooth swimmers.

Since there exists no mechanism for a decorrelation in the orientation of an isolated swimmer, (2.5) for the conservation of probability takes the simple form

$$\frac{\partial \Omega}{\partial t} + (U\,\boldsymbol{p} + \boldsymbol{u}) \cdot \nabla_x \Omega + \nabla_p \cdot (\dot{\boldsymbol{p}}\,\Omega) = 0, \tag{4.1}$$

the probability merely being convected along a phase-space trajectory; as in (2.6), the convection terms in physical and orientation space include both a mean-field contribution and one due to correlations. A non-interacting suspension of such swimmers has already been shown to be unstable at any non-zero concentration. Here by 'non-interacting', we mean the absence of any correlation between the positions or orientations of different bacteria; the ambient flow in the stability analysis is the mean-field driven by such uncorrelated orientation fluctuations of bacteria in the far field. The inclusion of correlations induced by hydrodynamic interactions will have several consequences. On account of pair-correlations, there will be a change in the swimming speed and a modification of the induced force density on a bacterium; the latter leads to a change in the magnitude of the destabilizing bacterial stress. There will also be hydrodynamically induced fluctuations in the centre-of-mass and orientation of a bacterium. Thus, $\dot{\boldsymbol{p}}$ in (4.1) must now include both a contribution due to the mean field, and one arising from the disturbance velocity field of a neighbouring bacterium, and the convection of probability ($\boldsymbol{u} \cdot \nabla_x \Omega$) must likewise account for the effect of the disturbance velocity fields due to neighbouring bacteria. We now argue that, in the dilute limit, the most important effect amongst all of the above is that of the orientation fluctuations. To begin with, observe that (4.1)

describes the (deterministic) evolution of probability on time scales of $O(L/U)$. On the other hand, the random nature of the hydrodynamic interactions for times much greater than $O(L/U)$ implies that the evolution equation on these time scales must contain terms representative of the appropriate stochastic decorrelation processes in position and orientation. The long-time evolution in physical space must evidently be diffusive; the orientation fluctuations and the resulting decorrelation in swimming motion, together with fluctuations in the centre-of-mass position, will give rise to a translational diffusivity. In the dilute limit, the frequency of pair interactions is $O(nUL^2)$, and the onset of a diffusive motion therefore occurs for times much greater than $O(nUL^2)^{-1}$. As already argued in § 3, the translation of a swimming bacterium, and the resulting convection of probability, becomes irrelevant in the limit of long-wavelength perturbations. The diffusive motion for times longer than $O(nUL^2)^{-1}$, and the resulting sampling of the inhomogeneous strain field associated with an imposed velocity perturbation, is even more inefficient in the limit $k \to 0$. A more accurate estimate may be obtained from the relevant Péclet number, defined as $Pe_t = U/(kD_t)$. Since the dominant contribution to translational diffusion arises from orientation fluctuations in the limit $nL^3 \ll 1$, and since a representative time scale for orientation decorrelation (t_r) is $t_r \sim O(nUL^2)^{-1}$, being related to the frequency of pair interactions, the translational diffusivity is given by $D_t \sim U^2 t_r \sim O(U/nL^2)$ (for a rotary diffusion process, $D_t = U^2/6D_r$; Brenner & Edwards 1993). Thus, $Pe_t \sim nL^2/k$, and $Pe_t \gg 1$ for $k \ll O(nL^2)$. Therefore, the term corresponding to translational diffusion in the equation for $\Omega(\boldsymbol{x}, \boldsymbol{p}, t)$ may be neglected in the limit of long wavelengths. Further, unlike the rotary diffusivity, the modifications in the induced force density, swimming speed, etc., in the limit $nL^3 \ll 1$, are $O(nL^3)$ smaller than their respective values in the absence of interactions. Thus, the most important effect of hydrodynamic interactions is the decorrelation due to the induced orientation fluctuations.

It will be seen later (see (4.2)) that the decorrelation in orientation of an otherwise straight swimmer occurs primarily on account of hydrodynamic interactions with neighbouring bacteria at a distance of the order of its own size. The resulting angular displacements are large in general, and a model for the related decorrelation process will involve non-local transport functions (see Shaqfeh & Koch 1988); this is, of course, similar to the decorrelation in orientation due to tumbling seen earlier in § 3, or the decorrelation in velocity due to collisions in hard-sphere gases (see Chapman & Cowling 1991). On the other hand, for sufficiently slender bacteria ($r \gg 1$), the disturbance velocity field driving the orientation fluctuations is weak. Now, for a smooth distribution of forces on a slender body, the velocity disturbance is only $O(\ln r)^{-1}$ on length scales of $O(L)$. This is, however, not the case for *E. Coli*, our main object of interest from the point of view of experimental verification, since the head of an *E. Coli* is close to being a spheroid with an aspect ratio of 2; in fact, the strength of the force dipole for an *E. Coli* was estimated in § 3 using this approximation for the shape of the head. Thus, the smallness of the velocity disturbance on length scales of $O(L)$ in this case is because the force dipole exerted by a swimming *E. Coli* consists of the drag exerted by the small head (with length $L_H \approx 0.2L$), and an equal and opposite propulsive force exerted along the much longer tail. Owing to its length, the force per unit length on the tail is smaller by a factor of $O(L_H/L)$, while the velocity disturbance generated by the blunt head decays on a length scale of $O(L_H)$ rather than L, and is again only $O(L_H/L)$ on length scales of $O(L)$. Since pair interactions that contribute dominantly to angular displacements occur at separations of $O(L)$, the angular displacement accompanying each pair interaction is again $O(L_H/L)$ and therefore small. The orientation fluctuations then evolve via a local diffusive process characterized by a hydrodynamic rotary diffusivity (D_r^h). It is

worth noting that the slender rods simulated by Saintillan & Shelly (2007) swim due to an actuating shear stress localized near the head (a puller) or tail (a pusher). The latter is similar to an *E. Coli*, and the orientation distribution in a stable suspension of such rods is again expected to evolve via a rotary diffusion process in the limit $nL^3 \ll 1$; the analysis below remains applicable to this system. On the other hand, the active swimmers in simulations of Hernandez *et al.* (2005) are modelled as point-force dipoles, and the resulting strongly singular velocity field will lead to qualitatively different interactions; in particular, the orientation dynamics in this case is likely to be dominated by the large changes in orientation accompanying the close approach of two or more swimmers.

The (nominal) scale for D_r^h may be obtained by noting that the rate of rotation due to the disturbance velocity field is $O(U/L)$, and that the characteristic time of interaction is $O(L/U)$. D_r^h is then given by the product of the mean squared angular displacement with the frequency of interactions; $D_r^h \sim O(nUL^2)$. Note that in the above scalings we have used only the nominal scale U/L for the velocity gradient, not accounting for the additional factor of (L_H/L) that would make this gradient, and the resulting angular displacements, small. For now, this smallness is implicit. The numerical pre-factor obtained later in a manner similar to § 3, that is, from an estimate for the drag on the head, will automatically account for the additional factor of $O(L_H/L)$, and thence, the smallness of the resulting rotary diffusivity. The above scale for the rotary diffusivity, together with the expression for the threshold concentration derived in the earlier section for rotary diffusing bacteria, now makes evident the non-trivial effect of pair-hydrodynamic interactions in the dilute limit. With $nL^3 \ll 1$, expression (3.7) for the threshold concentration for a suspension of smooth slender-bodied swimmers with $D_r = D_r^h$ reduces to $nUL^2/D_r^h = 30/C$. Using $D_r^h = k_r(nUL^2)$, the constant k_r being determined from the analysis that follows, we note that stability results if $k_r > C/30$. As already seen, $C \approx 0.57$ for *E. Coli*, and $(C/30)$ is rather a small number. There is thus a realistic possibility of even weak pair interactions stabilizing a suspension of slender bacteria in the dilute limit. Using the above scale for D_r^h, it is also seen that the ratio of the terms representing translational $(D_t \nabla_{\boldsymbol{x}}^2 \Omega)$ and rotary $(D_r^h \nabla_{\boldsymbol{p}}^2 \Omega)$ diffusion is $O(k/nL^2)$, and as argued above, translational diffusion may therefore be neglected in the limit $k \ll nL^2$.

We now proceed to calculate the hydrodynamic rotary diffusivity for slender bacteria arising from pair interactions. To do this, we must derive the required evolution equation containing the rotary diffusive term. We first write down (4.1), neglecting terms corresponding to convection in physical space and the translational diffusion contribution, as

$$\frac{\partial \Omega}{\partial t} + \nabla_{\boldsymbol{p}} \cdot \left(\left\{ \dot{\boldsymbol{p}}^m(\boldsymbol{x}, t) + n \int \dot{\boldsymbol{p}}^i(\boldsymbol{x}|C_2) \Omega'_{1|1}(C_2, t|\boldsymbol{x}, \boldsymbol{p}) \mathrm{d}C_2 \right\} \Omega \right) = 0. \tag{4.2}$$

Here, we have explicitly separated the contributions due to the mean field and correlated pair interactions, as in (2.11), and C_2 denotes the configuration $[\boldsymbol{x}_1, \boldsymbol{p}_1]$ of a second bacterium. The contribution to the bacterium rotation by the long-wavelength perturbations characterizing the mean-field remains correlated for times and lengths much longer than the contribution due to local pair-hydrodynamic interactions, and will therefore retain its (convective) form even for times much longer than $O(nUL^2)^{-1}$ when the interaction-contribution assumes a diffusive form. We also note that the integral representing the interaction contribution involves the product of a rotation $(\dot{\boldsymbol{p}}^i)$ due to a disturbance velocity field, and a perturbation

pair-probability ($\Omega'_{1|1}$), and therefore has its largest contributions at separations of $O(L)$, decaying rapidly thereafter. Since (4.2) requires knowledge of the perturbation to the conditional probability, $\Omega'_{1|1}(C_2, t|\boldsymbol{x}, \boldsymbol{p})$, we first write down the conservation equation for the pair-probability, $\Omega_2(\boldsymbol{x}, \boldsymbol{x}_1, \boldsymbol{p}, \boldsymbol{p}_1, t) = \Omega_{1|1}(C_2, t|\boldsymbol{x}, \boldsymbol{p})\Omega(\boldsymbol{p}, t)$, neglecting smaller, $O(nL^3)$, corrections due to three-body interactions

$$\frac{\partial \Omega_2}{\partial t} + U\,\boldsymbol{p}\cdot\nabla_{\boldsymbol{x}}\Omega_2 + U\,\boldsymbol{p}_1\cdot\nabla_{\boldsymbol{x}_1}\Omega_2 + \nabla_{\boldsymbol{p}}\cdot(\dot{\boldsymbol{p}}\,\Omega_2) + \nabla_{\boldsymbol{p}_1}\cdot(\dot{\boldsymbol{p}}_1\Omega_2) = 0. \tag{4.3}$$

For a slender bacterium, both the convection of probability, and the rotation of a bacterium by the disturbance velocity field are $O(L_H/L)$ smaller, and at leading order, the pair-probability is just convected along the quiescent swimming trajectories. Thus, $\Omega_2 = \Omega(\boldsymbol{p}, t)\Omega(\boldsymbol{p}_1, t)$ at leading order. We now expand the pair-probability as $\Omega_2 = \Omega(\boldsymbol{p}, t)\Omega(\boldsymbol{p}_1, t) + \Omega_2^{(1)} + \cdots$, where $\Omega_2^{(1)} = \Omega'_{1|1}(C_2, t|\boldsymbol{x}, \boldsymbol{p})\Omega(\boldsymbol{p}, t)$. Anticipating $\Omega_2^{(1)}$ to be $O(L_H/L)$ smaller, and further, noting that Ω_2 is only a function of the relative position $\boldsymbol{r} = \boldsymbol{x} - \boldsymbol{x}_1$, we find the following set of equations to $O(L_H/L)$:

$$\frac{\partial \Omega}{\partial t} + \nabla_{\boldsymbol{p}}\cdot(\dot{\boldsymbol{p}}^m\,\Omega) + n\nabla_{\boldsymbol{p}}\cdot\left(\int \dot{\boldsymbol{p}}^i(\boldsymbol{r}, \boldsymbol{p}\,|\boldsymbol{0}, \boldsymbol{p}_1)\Omega_2^{(1)}(\boldsymbol{r}, \boldsymbol{p}, \boldsymbol{p}_1)\,\mathrm{d}C_2\right) = 0, \tag{4.4}$$

$$U(\boldsymbol{p}-\boldsymbol{p}_1)\cdot\nabla_{\boldsymbol{r}}\Omega_2^{(1)} = -\big[\Omega(\boldsymbol{p}_1, t)\nabla_{\boldsymbol{p}}\cdot[\dot{\boldsymbol{p}}^i(\boldsymbol{r}, \boldsymbol{p}|\boldsymbol{0}, \boldsymbol{p}_1)\,\Omega(\boldsymbol{p}, t)] + \Omega(\boldsymbol{p}, t)\nabla_{\boldsymbol{p}_1}\cdot\big[\dot{\boldsymbol{p}}_1^i(-\boldsymbol{r}, \boldsymbol{p}_1|\boldsymbol{0}, \boldsymbol{p})\Omega(\boldsymbol{p}_1, t)\big]\big]. \tag{4.5}$$

In the above, we have implicitly assumed the pair-correlations contained in Ω_2 to evolve on a time scale much shorter than that characterizing the evolution of Ω itself, and thus, for times greater than $O(L/U)$, and of interest here, the time derivative in (4.5) may be neglected, with the consequence that the time dependence in Ω_2 always enters in an implicit manner via the singlet probability density (see Shaqfeh & Koch 1988). For the same reason, we have not considered a coupling in (4.3) of the slowly evolving perturbation with the relatively rapid pair interactions. Solving (4.5), one obtains

$$\Omega_2^{(1)} = -\int_{-\infty}^{r_U} \frac{\mathrm{d}r'_U}{U|\boldsymbol{p}-\boldsymbol{p}_1|}[\Omega(\boldsymbol{p}_1, t)\nabla_{\boldsymbol{p}}\cdot[\dot{\boldsymbol{p}}^i(\boldsymbol{r}', \boldsymbol{p}|\boldsymbol{0}, \boldsymbol{p}_1)\,\Omega(\boldsymbol{p}, t)] + \Omega(\boldsymbol{p}, t)\nabla_{\boldsymbol{p}_1}\cdot[\dot{\boldsymbol{p}}_1(-\boldsymbol{r}', \boldsymbol{p}_1|\boldsymbol{0}, \boldsymbol{p})\Omega(\boldsymbol{p}_1, t)]], \tag{4.6}$$

where r_U is a coordinate along the direction of relative translation; that is, $r_U = \boldsymbol{r}\cdot\hat{\boldsymbol{U}}$ with $\hat{\boldsymbol{U}} = (\boldsymbol{p}-\boldsymbol{p}_1)/|\boldsymbol{p}-\boldsymbol{p}_1|$. Using (4.6) in (4.4), and noting that there can be no rotational drift on account of symmetry (which will otherwise lead to an anisotropic orientation distribution even in the absence of an imposed flow), one finally obtains the following equation for $\Omega(\boldsymbol{p}, t)$:

$$\frac{\partial \Omega}{\partial t} + \nabla_{\boldsymbol{p}}\cdot(\dot{\boldsymbol{p}}^m\Omega) - n\,\nabla_{\boldsymbol{p}}\cdot\boldsymbol{D}_r^h\cdot\nabla_{\boldsymbol{p}}\,\Omega = 0, \tag{4.7}$$

where the (tensorial) hydrodynamic rotary diffusivity is given by the expression

$$\boldsymbol{D}_r^h = n\int \mathrm{d}C_2\,\Omega(\boldsymbol{p}_1, t)\int_{-\infty}^{r_U}\frac{\mathrm{d}r'_U}{U|\boldsymbol{p}-\boldsymbol{p}_1|}\dot{\boldsymbol{p}}^i(\boldsymbol{r}', \boldsymbol{p}\,|\boldsymbol{0}, \boldsymbol{p}_1)\dot{\boldsymbol{p}}^i(\boldsymbol{r}, \boldsymbol{p}\,|\boldsymbol{0}, \boldsymbol{p}_1). \tag{4.8}$$

We note that the integral over C_2 involves both a spatial ($\boldsymbol{r}$) and an orientational integral ($\boldsymbol{p}_1$). Choosing coordinates as $(\boldsymbol{r}^{\perp}, r_U) \equiv [\boldsymbol{r}\cdot(\boldsymbol{I}-\hat{\boldsymbol{U}}\hat{\boldsymbol{U}}), r_U]$ for the spatial integral, a simple integration by parts with respect to r_U (see Shaqfeh & Koch 1988) leads to

the following alternate symmetric and intuitive form:

$$\boldsymbol{D}_r^h = \frac{nUL^2}{2}\int \mathrm{d}\boldsymbol{p}_1 \Omega(\boldsymbol{p}_1, t)\int \frac{\mathrm{d}\boldsymbol{r}^{\perp}}{|\boldsymbol{p}-\boldsymbol{p}_1|}\int_{-\infty}^{\infty}\mathrm{d}r'_U \dot{\boldsymbol{p}}^i(\boldsymbol{r}', \boldsymbol{p}\,|\boldsymbol{0}, \boldsymbol{p}_1)\int_{-\infty}^{\infty}\mathrm{d}r''_U \dot{\boldsymbol{p}}^i(\boldsymbol{r}'', \boldsymbol{p}\,|\boldsymbol{0}, \boldsymbol{p}_1), \tag{4.9}$$

where the integral over $\boldsymbol{r}^{\perp}$ is one over the plane perpendicular to $\boldsymbol{U}$, and we have now used the scales L and U for lengths and velocities, respectively; we will continue to use dimensionless variables in the analysis that follows. One may now identify, in (4.9), each of the inner integrals over r_U as the net angular displacement accompanying a single (weak) pair interaction. It is convenient to evaluate the above expression in transform space. Following the same convention for the transform as in § 3, one obtains using the convolution theorem

$$\boldsymbol{D}_r^h = \frac{nUL^2}{2}\int \mathrm{d}\boldsymbol{p}_1 \Omega(\boldsymbol{p}_1, t)\int \mathrm{d}\boldsymbol{\xi}\,\frac{1}{|\boldsymbol{p}-\boldsymbol{p}_1|}\hat{\dot{\boldsymbol{p}}}^i(k_U=0, \boldsymbol{\xi})\hat{\dot{\boldsymbol{p}}}^i(k_U=0, -\boldsymbol{\xi}), \tag{4.10}$$

where $k_U = \boldsymbol{k}\cdot\hat{\boldsymbol{U}}$, and $\boldsymbol{\xi} = \boldsymbol{k}\cdot(\boldsymbol{I}-\hat{\boldsymbol{U}}\hat{\boldsymbol{U}})$ is the reciprocal vector in the plane transverse to $\hat{\boldsymbol{U}}$. The Fourier transform of the rotational velocity required in (4.10), $\hat{\dot{p}}(\boldsymbol{k})$, may now be determined by regarding the slender bacterium as a line distribution of forces. Note that this differs from our earlier treatment in § 3 where we approximated the rotation of a bacterium due to an imposed flow by that corresponding to a local linear flow owing to the separation of length scales between the bacterium size and the wavelength characterizing the mean-field fluctuations. This is not the case here, since as pointed out earlier, the dominant contribution to the rotary diffusivity occurs when the pair of bacteria is separated by $O(L)$, and the disturbance velocity field due to each bacterium (that causes the rotation) may not be approximated by a linear flow on this length scale. Therefore, we use the expression for the rotation of a slender body in an arbitrary imposed flow (for instance, see Rahnama *et al.* 1993). The imposed flow in our case is the disturbance velocity field of the second bacterium with orientation $\boldsymbol{p}_1$ located at $-\boldsymbol{r}$; the rotation of the given bacterium at the origin is given by

$$\dot{\boldsymbol{p}}^i(\boldsymbol{r}, \boldsymbol{p}\,|\boldsymbol{0}, \boldsymbol{p}_1) = \frac{3}{2}\int_{-1/2}^{1/2} s\,\mathrm{d}s(\boldsymbol{I}-\boldsymbol{pp})\cdot\boldsymbol{u}'(\boldsymbol{r}+s\boldsymbol{p}\,|\boldsymbol{0}, \boldsymbol{p}_1), \tag{4.11}$$

where $\boldsymbol{u}'(\boldsymbol{r}+s\boldsymbol{p}|\boldsymbol{0}, \boldsymbol{p}_1)$ is the disturbance velocity field due to the second bacterium evaluated along the axis of the given bacterium. In transformed variables, one obtains

$$\hat{\dot{\boldsymbol{p}}}(\boldsymbol{k}) = \frac{3\mathrm{i}}{4}(\boldsymbol{I}-\boldsymbol{pp})\cdot\hat{\boldsymbol{u}}(\boldsymbol{k}; \boldsymbol{p}_1) j_1(\pi\boldsymbol{k}\cdot\boldsymbol{p}), \tag{4.12}$$

where $j_1(z) = \sin z/z^2 - \cos z/z$ is the spherical Bessel function of the first kind (see Abramowitz & Stegun 1970). The expression for the Fourier transformed velocity disturbance may be obtained from an axial force distribution of a form used earlier for *E. Coli* in § 3. Thus, in dimensionless terms, $\boldsymbol{f}(s) = M^{-1}\boldsymbol{p}$ for $1/2-\alpha < s < 1/2$ and $\boldsymbol{f}(s) = -(\alpha/(1-\alpha))M^{-1}\boldsymbol{p}$ for $-1/2 < s < 1/2-\alpha$, where $\alpha = 0.2$ and the axial mobility coefficient M being given by (3.8); one obtains

$$\hat{\boldsymbol{u}}(\boldsymbol{k}; \boldsymbol{p}_1) = M\frac{\boldsymbol{p}_1\cdot(\boldsymbol{I}-\hat{\boldsymbol{k}}\hat{\boldsymbol{k}})}{(2\pi k)^2}\,\mathscr{U}(\pi\boldsymbol{k}\cdot\boldsymbol{p}_1), \tag{4.13}$$

where the function $\mathscr{U}(z)$ depends on the details of the bacterium force distribution. For the dependence assumed above, one finds

$$\mathscr{U}(z) = \frac{\mathrm{i}}{2z}\left[\frac{\alpha}{(1-\alpha)}\,\mathrm{e}^{\mathrm{i}z} + \mathrm{e}^{-\mathrm{i}z} - \frac{1}{(1-\alpha)}\,\mathrm{e}^{-z(1-2\alpha)}\right]. \tag{4.14}$$

The hydrodynamic rotary diffusivity tensor $\boldsymbol{D}_r^h$ must be of the form $D_r^h(\boldsymbol{I}-\boldsymbol{pp})$ since rotation of a swimmer about its axis of symmetry does not lead to a change in orientation. The scalar hydrodynamic rotary diffusivity D_r^h, that now replaces D_r in (2.5), for instance, is then given by $D_r^h = \frac{1}{2}(\boldsymbol{I}:\boldsymbol{D}_r^h)$. Thus,

$$D_r^h = \frac{nUL^2}{4}\int \mathrm{d}\boldsymbol{p}_1 \Omega(\boldsymbol{p}_1,t)\int \mathrm{d}\boldsymbol{\xi}\frac{1}{|\boldsymbol{p}-\boldsymbol{p}_1|}\hat{\boldsymbol{p}}^i(k_U=0,\boldsymbol{\xi})\cdot\hat{\boldsymbol{p}}^i(k_U=0,-\boldsymbol{\xi}). \tag{4.15}$$

Using (4.12) in (4.15), one obtains

$$D_r^h = \frac{9nUL^2}{64}\int \mathrm{d}\boldsymbol{p}_1 \Omega(\boldsymbol{p}_1,t)\int \mathrm{d}\boldsymbol{\xi}\frac{1}{|\boldsymbol{p}-\boldsymbol{p}_1|}[j_1(\pi\boldsymbol{\xi}\cdot\boldsymbol{p})]^2 \times \hat{\boldsymbol{u}}(k_U=0,\boldsymbol{\xi};\boldsymbol{p}_1)\cdot(\boldsymbol{I}-\boldsymbol{pp})\cdot\hat{\boldsymbol{u}}(k_U=0,-\boldsymbol{\xi};\boldsymbol{p}_1). \tag{4.16}$$

Choosing a coordinate system in the plane perpendicular to $\hat{\boldsymbol{U}}$ spanned by the unit vectors $\boldsymbol{e}_1=\boldsymbol{p}\wedge\boldsymbol{p}_1/|\boldsymbol{p}\wedge\boldsymbol{p}_1|$ and $\boldsymbol{e}_2=(\boldsymbol{I}-\hat{\boldsymbol{U}}\hat{\boldsymbol{U}})\cdot\boldsymbol{p}_1/|(\boldsymbol{I}-\hat{\boldsymbol{U}}\hat{\boldsymbol{U}})\cdot\boldsymbol{p}_1|$, we have $\boldsymbol{\xi}=\xi_1\boldsymbol{e}_1+\xi_2\boldsymbol{e}_2$; Further, using $\boldsymbol{p}\cdot\boldsymbol{p}_1=\cos\theta_p$, one obtains

$$D_r^h = (nUL^2)\frac{9M^{-2}}{1024\pi^4}\int \mathrm{d}\boldsymbol{p}_1\frac{\Omega(\boldsymbol{p}_1,t)}{\sqrt{2(1-\cos\theta_p)}}\int \mathrm{d}\xi_1 d\xi_2\frac{1}{\xi^4}[j_1(\pi\xi_2 p_2)]^2\mathscr{U}(\pi\xi_2 p_2) \times \mathscr{U}(-\pi\xi_2 p_2)[\boldsymbol{p}_1\cdot(\boldsymbol{I}-\hat{\boldsymbol{\xi}}\hat{\boldsymbol{\xi}})\cdot(\boldsymbol{I}-\boldsymbol{pp})\cdot(\boldsymbol{I}-\hat{\boldsymbol{\xi}}\hat{\boldsymbol{\xi}})\cdot\boldsymbol{p}_1], \tag{4.17}$$

where $\xi^2=\xi_1^2+\xi_2^2$ and $p_2=(1/2)\sqrt{(1+\cos\theta_p)}$. Again, exploiting the rapidity of pair interactions relative to the time scale of evolution of any imposed long-wavelength perturbation, one may assume an isotropic distribution for the orientation of the interacting second bacterium; that is $\Omega(\boldsymbol{p}_1)=1/4\pi$. Evaluating the orientation integral in a spherical coordinate system with the polar axis along $\boldsymbol{p}$, further simplification gives

$$D_r^h = (nUL^2)\frac{9M^{-2}}{2048\pi^4}\int_0^\pi \mathrm{d}\theta_p\frac{\sin\theta_p}{\sqrt{2(1-\cos\theta_p)}}\int \mathrm{d}\xi_1 d\xi_2\frac{1}{\xi^4}[j_1(\pi\xi_2 p_2)]^2|\mathscr{U}(\pi\xi_2 p_2)|^2 \times \left[\sin^2\theta_p+(2\cos\theta_p-1)\frac{(\xi_2 p_2)^2}{\xi^2}-\frac{(\xi_2 p_2)^4}{\xi^4}\right], \tag{4.18}$$

with

$$|\mathscr{U}(\pi\xi_2 p_2)|^2 = \frac{1}{(1-\alpha)^2(2\pi\xi_2 p_2)^2}[(\cos(\pi\xi_2 p_2)-\cos[(1-2\alpha)\pi\xi_2 p_2])^2 + ((1-2\alpha)\sin(\pi\xi_2 p_2)-\sin[(1-2\alpha)\pi\xi_2 p_2])^2]. \tag{4.19}$$

With $\alpha=0.2$, the integrals over ξ_1 and ξ_2 may be evaluated to obtain, after some algebra,

$$D_r^h = 3\times 10^{-5}M^{-2}(nUL^2)\int_{-1}^{1}\mathrm{d}x\frac{(1+x)}{2^{3/2}(1-x)^{1/2}} \times \left[\frac{(1-x^2)}{4}+\frac{3(2x-1)(1+x)}{32}-\frac{5(1+x)^2}{128}\right], \tag{4.20}$$

where $x=\cos\theta_p$. Finally, calculating the above one-dimensional integrals, we have $D_r\approx k_r(nUL^2)$ with $k_r=2.9\times10^{-6}M^{-2}$. This value of k_r remains much too small when compared to $C/30$ for *E. Coli*; for instance, $C\approx0.57$, $M^{-1}\approx5.7$ (see (3.8)), and one obtains $C-/30\approx1.9\times10^{-2}$, and $k_r\approx9.4\times10^{-5}$. Thus, the rate of orientation decorrelation on account of relatively weak pairwise interactions is not large enough

to stabilize a dilute suspension of *E. Coli*. Owing to the smallness of k_r, this is very likely the case for any slender-bodied swimmer, and a weakly interacting suspension of slender-bodied swimmers is therefore expected to be unstable at any finite concentration. We do note, however, that the time scale characterizing the rate of accumulation of destabilizing stress starts to increase rapidly as the bacterium aspect ratio approaches unity since the effect of the ambient extension on the orientation of the bacterium becomes vanishingly small. On the other hand, the rate of orientation decorrelation must increase since the disturbance velocity fields are stronger for bacteria of a moderate aspect ratio, and the corresponding angular displacement, on account of hydrodynamic interactions, is larger. Therefore, it does appear as if a suspension of active particles, in the absence of any intrinsic orientation decorrelation mechanisms (as has been the case in simulations of active particles thus far), must, for a certain critical aspect ratio greater than unity, become stable to infinitesimal perturbations with vanishingly small wavenumbers. Such a suspension must then either be unconditionally stable or exhibit a finite wavelength cutoff for unstable perturbations.

5. Discussion

The analysis in the earlier sections has led to a host of expressions for the threshold concentration ($(nL^3)_{crit}$) in various limits of specific decorrelation mechanisms being dominant. It is therefore worthwhile providing a summary of the main results before putting our analysis into perspective in light of earlier theoretical efforts. We begin with the simplest case: a suspension of non-interacting 'straight swimmers' is always unstable owing to the absence of any orientation decorrelation mechanism. Thus, for this case $(nL^3)_{crit} = 0$. Next, with only rotary diffusion leading to orientation decorrelation, we find the following expression for the threshold concentration in a suspension of smooth swimmers:

$$(nL^3)_{crit} = \frac{\dfrac{30}{C\mathscr{F}(r)}\left(\dfrac{D_r L}{U}\right)}{\left(1 - \dfrac{15\mathscr{G}(r)}{C\mathscr{F}(r)}\left(\dfrac{D_r L}{U}\right)\right)}. \tag{5.1}$$

With random tumbling acting to decorrelate orientations instead, we obtain

$$(nL^3)_{crit} = \frac{\dfrac{5}{C\mathscr{F}(r)}\left(\dfrac{L}{U\tau}\right)}{\left(1 - \dfrac{5\mathscr{G}(r)}{2C\mathscr{F}(r)}\left(\dfrac{L}{U\tau}\right)\right)}. \tag{5.2}$$

With both rotary diffusion and random tumbling included, one finds:

$$(nL^3)_{crit} = \frac{\dfrac{30}{C\mathscr{F}(r)}\left(\dfrac{D_r L}{U}\right)\left[1 + \dfrac{1}{6\tau D_r}\right]}{\left\{1 - \dfrac{15\mathscr{G}(r)}{C\mathscr{F}(r)}\left(\dfrac{D_r L}{U}\right)\left[1 + \dfrac{1}{6\tau D_r}\right]\right\}}. \tag{5.3}$$

This is the result quoted in the abstract, and it remains a very good approximation even in cases where the tumbles are not perfectly random as is the case with *E. Coli*. Finally, for the most general case of rotary diffusion and correlated tumbling, the

correlation parameter β being as defined in § 2, one finds

$$(nL^3)_{crit} = \frac{\dfrac{30}{C\mathscr{F}(r)}\left(\dfrac{D_r L}{U}\right)\left[1+\dfrac{1}{2\tau D_r}\dfrac{(\beta\cosh\beta-\sinh\beta)}{\beta^2\sinh\beta}\right]}{\left\{1-\dfrac{15\mathscr{G}(r)}{C\mathscr{F}(r)}\left(\dfrac{D_r L}{U}\right)\left[1+\dfrac{1}{2\tau D_r}\dfrac{(\beta\cosh\beta-\sinh\beta)}{\beta^2\sinh\beta}\right]\right\}}. \tag{5.4}$$

In each of the above cases, the threshold concentration diverges when the denominator vanishes. This condition then serves as a threshold for the rapidity of the relevant decorrelation mechanism(s). For faster rates of decorrelation, the bacterial suspension behaves in a manner similar to a suspension of passive particles. In the general case, the effective viscosity in this stable regime is given by

$$\mu_{eff} = \mu\left[1+\frac{(nL^3)\mathscr{G}(r)}{2}\left(1-\frac{\dfrac{C\mathscr{F}(r)}{15\mathscr{G}(r)}\left(\dfrac{U}{D_r L}\right)}{\left[1+\dfrac{1}{2\tau D_r}\dfrac{(\beta\cosh\beta-\sinh\beta)}{\beta^2\sinh\beta}\right]}\right)\right]. \tag{5.5}$$

The functions $\mathscr{F}(r)$ and $\mathscr{G}(r)$ appearing in the above expressions depend on the shape of the bacterium. For a spheroid of aspect ratio r, $\mathscr{F}(r)=(r^2-1)/(r^2+1)$; the corresponding expression for $\mathscr{G}(r)$, although more cumbersome, is available from standard sources (see Kim & Karrila 1991). The constant C denotes the non-dimensional strength of the bacterial force dipole, and is thus determined by the detailed spatial dependence of the force density exerted by a swimming bacterium. For the case of *E. Coli*, the aspect ratio being large, we obtain more specific predictions below by using $\mathscr{F}(r)\approx 1$, $\mathscr{G}(r)\approx \pi/45(\ln r)$; the specific value of C ($=0.57$) in this case was estimated in § 3 (see the text between (3.10) and (3.11)).

As discussed in § 1, ample evidence for the existence of a hydrodynamic instability in suspensions of swimming bacteria has emerged in the form of experimental observations of jets and vortical patterns (Mendelson *et al.* 1999; Dombrowski *et al.* 2004), enhanced diffusion of bacteria (Wu *et al.* 2006), colloidal beads (Wu & Libchaber 2000) and chemical tracers (Kim & Breuer 2004) and fluctuations in the force exerted on a bead held in an optical trap (Soni *et al.* 2003) within a bacterial suspension. The theory developed here suggests that convective motions should arise in bacterial suspensions above a critical concentration $(nL^3)_{crit}$ that depends on the length L, swimming speed U, tumbling frequency τ^{-1}, rotary diffusivity D_r and the force dipole $C\mu UL^2$, of a single swimming bacterium. The stability analysis predicts correlated orientation fluctuations on lengths scales much longer than the size of a single bacterium; the resulting anisotropic active stress drives fluid motion on the same scale, in turn implying increased velocity fluctuations in such a system. The fluid motion is expected to eventually grow to an amplitude where the convection of the orientation field fluctuations by the fluid motion (not included in the linearized analysis) would become comparable to that by the quiescent swimming speed, leading to correlated swimming over long length scales.

Returning to the case of an *E. Coli*, we note that the bacterium has a total length of about 10 μm, and an average duration between tumbles of about a second. Swimming speeds ranging from 10 to 30 $\mu m\,s^{-1}$ have been reported (Berg 2000; Wu *et al.* 2006). Berg (1983) estimated $D_r = 0.062\,s^{-1}$ by observing the curvature of a trajectory of wild-type *E. Coli* during a run. Wu *et al.* (2006) measured the translational diffusivity of smooth-swimming mutants, obtaining $D_t = 460\,\mu m^2\,s^{-1}$ and $U = 11\,\mu m\,s^{-1}$ for a dilute suspension ($n = 10^7$ cells $(ml)^{-1}$). Again using the

well-known relation $D_t = U^2/(6D_r)$ (see Brenner & Edwards 1993), for the long-time translational diffusivity, one finds $D_r = 0.042\,\mathrm{s}^{-1}$. The above estimate $C \approx 0.57$, for the dimensionless dipole strength for *E. Coli* was based on the drag on its head. However, experimental observations of the velocity correlation between neighbouring cells indicate a functional dependence on inter-particle separation that is in agreement with theory, but a magnitude that is about six times larger than a theoretical prediction based on the aforementioned drag estimate (see Liao *et al.* 2007). It is thus possible that C is larger than the above estimate by a factor of around 6. The above parameter values yield critical values of nL^3 in the range 0.7–3.5 for smooth swimmers and 4–16 for tumbling bacteria if one uses the theoretical estimate $C = 0.57$. The critical nL^3 would, however, be reduced to 0.1–0.5 for smooth swimmers, and 0.6–2 for tumbling bacteria if C was to be increased by a factor of 6 in view of the larger than expected velocity correlation of neighbouring bacteria. Wu *et al.* (2006) reported translational diffusivities of both wild-type and smooth-swimming *E. Coli* at $nL^3 \approx 0.2$ that were significantly greater than those observed in dilute suspensions suggesting the possibility that the threshold concentration may be as small or smaller than the estimate based on an enhanced force dipole ($C = 3.4$). The observed increase in the diffusivity of the smooth-swimming bacteria was larger than that for bacteria that tumble as might be expected on the basis of the earlier onset of instability predicted for smooth-swimming bacteria. It must nevertheless be mentioned that some of the above estimates for the hydrodynamic volume fraction (nL^3) are quite large, and one may question the applicability of a dilute analysis in this regime. We address this issue below when comparing our analysis with recent theoretical efforts.

Amongst the difficulties in achieving a more quantitative comparison of our predictions with experiments that have been performed to date are: (i) The bacterial concentration is often not known with precision and is varied in coarse increments; (ii) The swimming speed may vary depending on the bacterial strain and the procedure used to culture the bacteria; and (iii) The strength of the force dipole (as, for instance, indicated by the fluid velocity disturbance produced by a single cell) has not been measured experimentally. Previous experimental studies have focused primarily on characterizing the collective motion of bacteria when it occurs. The present study may encourage experimental investigators to determine when collective motion does and does not occur and seek a better understanding as to why it occurs. Numerical simulations that include bacterial tumbling and rotary diffusion would play a valuable role in bridging the gap between stability analysis and experiments.

We now put our analysis in perspective by looking at some recent simulations and theoretical efforts exploring the hydrodynamics of active particle suspensions. The stability of such suspensions was first analysed by Simha & Ramaswamy (2002) based on a mean-field description that included an expression for the stress exerted by the swimming particles acting as force dipoles. They considered an initially ordered system (an 'active nematic'), and proceeded to show that such nematic order is always susceptible to long-wavelength fluctuations, leading to eventual orientational disorder. Although a nematic phase is expected to arise only at much higher concentrations than those relevant to the analysis in this paper, the equations governing stability in the authors' mean-field description remain essentially the same, and the mechanism of instability thus remains the same as the one described in this paper. Indeed, it is easily seen from figure 3 that even an initially aligned suspension of swimmers, when subjected to a velocity perturbation in the form of a Fourier mode, will cause a reorientation of the intrinsic force dipoles that reinforces the original perturbation. In fact, the reinforcement is greatest when the swimmers are already aligned along the local extensional axis of the velocity wave, a situation that occurs for velocity waves

making an angle of 45° with the direction of initial alignment; this was the most unstable configuration found by the authors. Simha and Ramaswamy considered both polar and apolar suspensions of aligned swimmers. The absence of fore-aft symmetry in the former case leads to a net drift velocity even in the homogeneous base state. For the same reason, imposed velocity perturbations lead to both orientation and number density fluctuations, and the number density fluctuations were found to be anomalously large with $\langle(\delta N)^2\rangle/N \propto N^{2/3}$. In the context of the bacterial suspension examined here, the distinction between the polar and apolar cases is related to the symmetry of the base-state orientation distribution rather than the symmetry of an individual swimmer. Thus, an apolar bacterial suspension corresponds to an initial orientation distribution that is an even function of $\boldsymbol{p}$. As seen from the analysis in earlier sections, such a suspension does not admit number density fluctuations in the linear approximation. An example of a polar bacterial suspension occurs in the presence of a chemoattractant, where the direction of the chemoattractant gradient breaks the $\boldsymbol{p} \leftrightarrow -\boldsymbol{p}$ symmetry.

Saintillan & Shelley (2007) carried out numerical simulations of self-locomoting slender rods over a range of nL^3, where the rods were modelled as line distributions of forces, and hydrodynamic interactions between rods were treated using slender-body theory. The rods did not tumble, and the observed rotary diffusion was the result of multi-body hydrodynamic interactions. The simulations confirmed the prediction by Simha and Ramaswamy of a long-wavelength instability for an active nematic. The authors also obtained information concerning pair-correlations as a function of nL^3, and in particular, found a local nematic ordering to persist at shorter length scales on account of hydrodynamic interactions, even while there are unstable fluctuations in orientation on larger length scales. Further, Saintillan & Shelley (2007) plot the rotary diffusivity as a function of nL^3, and find a linear growth at small nL^3. As already seen in § 4, and also noted by the said authors, this linear increase appears consistent with the dominance of pair interactions, leading to a D_r of $O(nUL^2)$. There is a corresponding regime in their plot for the translational diffusivity, exhibiting an inverse scaling with nL^3 ($D_t \sim O(U/nL^2)$ (see § 4), again apparent characteristic of a dilute limit dominated by pair interactions. Both diffusion coefficients have a hydrodynamic origin, since the simulations did not incorporate any non-hydrodynamic decorrelation mechanisms. In fact, D_r continues to increase linearly, and D_t vary inversely, with nL^3 up to an $nL^3 \approx 10$. From figure 5 of their paper, we find that $D_r \approx 0.01\, nUL^2$, while for *E. Coli*, the analysis in § 4 gives $D_r \approx 9.4 \times 10^{-5} nUL^2$, a much smaller value. It must be noted that Saintillan & Shelley (2007) do not give the distribution of their actuating force; neither do they mention the aspect ratio of the swimming rods. Regardless, one expects the magnitude of the force dipole (C) in units of μUL^2 to be $O(1)$ for any reasonable force distribution. Thus, the discrepancy between the magnitudes of the two estimates suggests that the large rotary diffusivities extracted from the simulations may be a measure of the amplitude and length scales of the unstable velocity fluctuations rather than a manifestation of pair interactions in the dilute limit.

Recent simulations of active suspensions have also considered spherical swimmers; for instance, Ishikawa, Locsei & Pedley (2008) and Mehandia and Nott (2008) perform Stokesian dynamics simulations for spherical bacteria. As noted in § 2, the function $\mathscr{F}(r) \to 0$ in the limit of spherical particles since a sphere only responds to the vorticity in the ambient flow, and the resulting orientation distribution is therefore isotropic even in the presence of a shearing flow. This difference in orientation behaviour has a direct implication for the stability of a suspension of such swimmers. It is readily seen from the above expressions for $(nL^3)_{crit}$ that the threshold concentration in each

case diverges for spherical particles. Thus, it appears that correlated motion observed in the above simulations may have a different physical origin. The dynamics in these simulations is, in fact, quite sensitive to the nature of the near-field interactions. Mehandia & Nott (2008) find lubrication interactions to play a crucial role in the formation of clusters. Amongst other findings, the velocity distribution of the swimmers is Gaussian with full hydrodynamic interactions, while inclusion of far-field interactions alone leads to a sharply peaked distribution at the swimming speed. Further, even at the lowest concentrations, the authors find clusters consisting of swimmers in close proximity, again highlighting the role of lubrication interactions. Finally, in contrast to the findings of Wu *et al.* (2006), the translational diffusivity is found to decrease with increasing concentration. The sensitivity to the nature of near-field hydrodynamics may also play a role in the simulations of Ishikawa *et al.* (2008). The authors rely on a spherical 'squirmer' with a specified surface velocity distribution as a model for a swimming bacterium. Many of their results, including the peculiar nature of pair interactions (see Ishikawa, Simmonds & Pedley 2006) appear to be driven by the choice of surface velocity distribution. The dilatational nature of the surface velocity implies a strong radial inflow in the vicinity of a given squirmer, and thereby provides a natural clustering mechanism. The squirmer model is probably a reasonable representation for a ciliated organism such as Opalina, but by no means universal. One may, in fact, question the choice of the surface velocity boundary condition chosen by Ishikawa *et al.* (2006) even in the context of a ciliated organism. For these organisms, the cilia normally beat in a single direction, and one would therefore expect the (tangential) surface velocity to be single signed. However, the simplest approximation for such a velocity generates a potential flow without a force dipole, and Ishikawa *et al.* (2006) therefore included an additional contribution that does generate a force dipole but additionally leads to a reversal in direction of the surface velocity at a critical angle. Thus, it appears as if the correlated motion and clustering dynamics in suspensions of spherical swimmers may be largely driven by the nature of near-field interactions, and are at best specific to certain classes of swimmers. On the other hand, the instability investigated here is only related to the more universal nature of the long-ranged hydrodynamic interactions, and is therefore expected to be relevant to a wide class of micro-organisms.

The most relevant theoretical effort is that of Saintillan & Shelley (2008) who in addition to generalizing the analysis of Simha & Ramaswamy (2002) for an aligned suspension of active rods, also examined the stability of an initially isotropically oriented suspension of such swimmers. The governing equations, and the resulting stability characteristics of long-wavelength perturbations, are essentially the same as that for the suspension of straight swimmers examined here. In fact, even their eigenspectrum is identical to the results of our finite wavelength analysis (again, for straight swimmers) to be presented in a forthcoming publication (Subramanian & Koch in press). There is, however, little discussion of the underlying physics in this paper, the origin of the instability being merely attributed to active shear stresses. The physical explanation for the instability mechanism in such a suspension of straight swimmers has since been clarified by Underhill, Hernandez Ortiz & Graham (2008), who note, as we did in § 1, that the instability essentially arises due to the opposing nature of the induced and intrinsic force dipoles for a pusher. More importantly, the absence of any orientation decorrelation mechanisms in the above analyses implies that the suspension of self-propelled rods is always unstable. The inclusion of both a rotary diffusivity and correlated tumbling in our analysis not only makes it a more accurate model for suspensions of real bacteria, but more importantly, demonstrates the existence of a threshold concentration for the onset of an instability.

The detailed physical arguments presented here help clarify the physical origin of the instability. Saintillan & Shelley (2008) do include a translational diffusivity in their stability analysis; however, this term is of $O(k^2)$ in the limit $k \to 0$, and thence asymptotically small compared to the $O(k)$ convection of probability by the swimming velocity. The latter was already shown to be unimportant in the determination of the neutral curve, and therefore, translational diffusion will not lead to a threshold concentration. In any event, the allowance for a centre-of-mass diffusion in the absence of a rotary diffusivity is inconsistent, since the natural coupling that arises between orientation fluctuations and the resulting decorrelation in swimming motion is absent. By including a stress contribution that reflects the resistance of a bacterium to the deforming action of an ambient flow, we have also shown the transition in behaviour of a dilute bacterial suspension to the familiar well-analysed case of a suspension of passive particles. Finally, we have also highlighted the non-trivial effect of pair-hydrodynamic interactions in a suspension of self-propelled particles when intrinsic decorrelation mechanisms such as tumbling are absent. It is possible for a suspension of such swimmers to be stabilized by an interaction-driven orientation decorrelation, although we find that the actual rate of decorrelation is too small in the limit of slender rods. This is confirmed by the simulation results of Saintillan & Shelley (2007) who always find a suspension of interacting swimming rods to be unstable in the range of concentrations investigated.

We finally turn to the important point of determining the range of validity of the present stability analysis, and the resulting prediction for the threshold concentration. Recalling the scaling arguments discussed at the beginning of § 3 in terms of a generic correlation time t_{corr}, we observe that instability occurs when $t_{corr} = (1/nUL^2)[1 + nL^3\mathscr{G}(r)/2]$, in turn implying a threshold concentration for instability given by

$$(nL^3)_{crit} = \frac{\dfrac{L}{Ut_{corr}}}{\left[1 - \dfrac{L}{Ut_{corr}}\dfrac{\mathscr{G}(r)}{2}\right]}.$$

Evidently, the present analysis and the underlying assumption of diluteness become rigorously valid in the limit $Ut_{corr}/L \gg 1$, when $nL^3 \sim O(L/Ut_{corr}) \ll 1$. This is certainly the case in simulations of dilute suspensions of active swimmers wherein the orientation decorrelation occurs only due to occasional pair-hydrodynamic interactions; the relevant time scale for decorrelation is $O(nUL^2)^{-1}$, this being the frequency of uncorrelated pair interactions, and (Ut_{corr}/L) is therefore asymptotically large. Indeed, it was shown in § 4 that such a suspension of weakly interacting swimming rods is unstable at any non-zero concentration however small. For a suspension of real bacteria such as *E. Coli* the earlier numerical estimates certainly suggest that $(nL^3)_{crit}$, particularly for the case of wild-type tumblers, might be $O(1)$, thereby bringing into question the applicability of a dilute theory to experiments. However, two well-known instances of passive-particle suspension behaviour suggest otherwise. The first is a suspension of passive Brownian fibres in which case it is known that the rotary diffusivity of a Brownian fibre starts to decrease steeply only beyond an nL^3 of about 30 due to the confining-tube effect characteristic of a semi-dilute regime ($D_r \propto (nL^3)^{-2}$ for larger nL^3; see Larson 1988); although, in principle, the dilute regime with a constant D_r (equal to the Stokes–Einstein value for an isolated fibre) must prevail for only $nL^3 < 1$. The second instance is the case of non-Brownian fibre suspensions; in a series of articles (see Mackaplow, Shaqfeh & Schiek 1994; Mackaplow & Shaqfeh 1996, 1988), Mackaplow and Shaqfeh have

examined the transport of heat and mass, rheology and the mean sedimentation speed in these systems. Their results indicate that the dilute theory continues to give a reasonable estimate for $nL^3 \sim O(1)$. For instance, the plot for the normalized thermal conductivity in Mackaplow *et al.* (1994) shows only a 10 % deviation from its value at infinite dilution for $nL^3 \approx 5$. At the same value of nL^3, the mean sedimentation speed for an isotropic orientation distribution calculated by Mackaplow & Shaqfeh (1998) shows a modest reduction of about 20 %. The results of Mackaplow & Shaqfeh (1996) again show that the normalized stress in suspensions of both aligned and isotropically oriented non-Brownian fibres exhibits a modest deviation of about 20 % from the dilute estimate up to an $nL^3 \approx 10$. Clearly, there is no fundamental difference in the nature of hydrodynamic interactions in a suspension of active or passive slender rods. For the case of 'pushers', however, the existence of an instability in the dilute limit obscures the dynamics of interactions, as is evident from the simulations of Saintillan & Shelley (2007). On the other hand, it is likely that in a suspension of 'pullers' interactions come into play in the same qualitative manner as they do in a Brownian fibre suspension. Thus, one would expect D_r to increase linearly with nL^3 for small nL^3, while at higher nL^3 this increase may be offset due to the competing effects of (screened) hydrodynamic interactions driving orientation fluctuations and a tube-confinement effect. More importantly, one again expects the dynamics to differ qualitatively from a dilute scenario only beyond an nL^3 significantly larger than unity. Based on the above discussion, we therefore expect the stability analysis carried out in this paper to remain quantitatively accurate, and therefore relevant to suspensions of slender bacteria with $nL^3 \sim O(1)$.

In the dilute regime, there are $O(nL^3)$ contributions arising from pair interactions including a variation in the induced force–density, a change in the mean swimming speed, etc. The aforementioned simulations of Saintillan and Shelley have examined some of these effects, but they are beyond the scope of the present analysis. Herein, we have focused solely on the effects of pair interactions that remain significant even in the limit $nL^3 \ll 1$. The dominant effect was found to be an interaction-induced decorrelation in orientation affecting the dynamics of long-wavelength perturbations. It was shown in § 4 that this decorrelation in orientation is a diffusive process for slender bacteria; the resulting hydrodynamic rotary diffusivity was found to be too small to alter the stability characteristics of long-wavelength perturbations. In light of the above discussion on the transport characteristics of passive particle suspensions and their relation to the corresponding dilute estimates, however, we note that the other effects related to pair-correlations are likely to be small for $nL^3 \sim O(1)$. The pair-distribution function characterizing correlations in position and orientation in a suspension of slender bacteria, and the resulting implications, at higher nL^3, for the stability analysis carried out here will be reported in a future publication.

Appendix A: Derivation of the averaged equations for a bacterial suspension

The derivation of the averaged equations ((2.1) and (2.2)) for a suspension of neutrally buoyant bacteria is given herein. A derivation in the same spirit, but not explicitly accounting for hydrodynamic interactions, has been given by Simha & Ramaswamy (2002). We first write down the equations governing the motion of the Newtonian suspending fluid for a given configuration of the N swimming bacteria. If $[\boldsymbol{x}^\alpha, \boldsymbol{p}^\alpha]_{\alpha=1}^N$ be the positions and orientations of the N bacteria, then, in the absence of inertial effects, the velocity ($\boldsymbol{u}$) and pressure fields (p) in the suspending fluid satisfy the quasi-steady Stokes equations, and the fluid motion is completely determined

by the instantaneous motion of the swimming bacteria. For convenience, we restrict ourselves to the case of slender bacteria which may be treated as line distributions of forces. With this approximation, the no-slip boundary conditions on the bacterial surfaces may be directly incorporated as forcing terms in the Stokes equations. Thus, one obtains

$$\mu\nabla^2\boldsymbol{u} - \nabla p + \sum_{\alpha=1}^{N}\int_{-L/2}^{L/2} \boldsymbol{f}^{\alpha}(s, [\boldsymbol{x}^{\alpha}, \boldsymbol{p}^{\alpha}]; [\boldsymbol{x}^{\beta}, \boldsymbol{p}^{\beta}]_{\beta=1(\beta\neq\alpha)}^{N})\delta(\boldsymbol{x}-\boldsymbol{x}^{\alpha}-s\boldsymbol{p}^{\alpha})\,\mathrm{d}s = \boldsymbol{0}. \quad \text{(A 1)}$$

We have assumed all bacteria to have the same length L, and in the interests of notational simplicity, used s to denote the arclength coordinate along all N bacteria. $\boldsymbol{f}^{\alpha}(s, [\boldsymbol{x}^{\alpha}, \boldsymbol{p}^{\alpha}]; [\boldsymbol{x}^{\beta}, \boldsymbol{p}^{\beta}]_{\beta=1(\beta\neq\alpha)}^{N})$ is the linear force density exerted by the αth bacteria located at $\boldsymbol{x}^{\alpha}$ with orientation $\boldsymbol{p}^{\alpha}$. Aside from the obvious dependence on $[\boldsymbol{x}^{\alpha}, \boldsymbol{p}^{\alpha}]$, the force density, on account of hydrodynamic interactions, also depends on the configurations of all other swimming bacteria. For $\boldsymbol{f}^{\alpha}$, this dependence is explicitly indicated by the factor $[\boldsymbol{x}^{\beta}, \boldsymbol{p}^{\beta}]_{\beta=1^{N}(\beta\neq\alpha)}$. Since even an isolated bacterium swimming in an unbounded quiescent fluid exerts a force density $\boldsymbol{f}^{b}(\boldsymbol{s}, \boldsymbol{p}^{\alpha})$, it is convenient to first separate this part of the force density from the part ($\boldsymbol{f}'$) that arises solely on account of hydrodynamic interactions with neighbours; an example of the latter would be the force dipole (stresslet) induced in a given bacterium by the disturbance velocity field generated by its neighbours. Equation (A 1) may therefore be rewritten as

$$\mu\nabla^2\boldsymbol{u} - \nabla p + \sum_{\alpha=1}^{N}\int_{-L/2}^{L/2} [\boldsymbol{f}^{b}(s; \boldsymbol{x}^{\alpha}, \boldsymbol{p}^{\alpha}) + \boldsymbol{f}'^{\alpha}(s; [\boldsymbol{x}^{\alpha}, \boldsymbol{p}^{\alpha}]; \times [\boldsymbol{x}^{\beta}, \boldsymbol{p}^{\beta}]_{\beta=1(\beta\neq\alpha)}^{N})]\delta(\boldsymbol{x}-\boldsymbol{x}^{\alpha}-s\boldsymbol{p}^{\alpha})\,\mathrm{d}s = \boldsymbol{0}, \quad \text{(A 2)}$$

where the additional position dependence in $\boldsymbol{f}^{b}$ may arise on account of an imposed flow. Since our aim is to extract a continuum description of the system in terms of averaged fields, the implicit assumption is one of looking at length scales that are much larger than the typical size of a microstructural unit – in this case the size of a bacterium. Keeping this in mind, one may (formally) expand the delta functions in (A 2) about the geometric centre of each bacterium ($\boldsymbol{x}^{\alpha}$). Thus, using $\delta(\boldsymbol{x}-\boldsymbol{x}^{\alpha}-s\boldsymbol{p}^{\alpha}) = \delta(\boldsymbol{x}-\boldsymbol{x}^{\alpha}) - s\boldsymbol{p}^{\alpha}\cdot\nabla\delta(\boldsymbol{x}-\boldsymbol{x}^{\alpha}) + \frac{s^2}{2}\boldsymbol{p}^{\alpha}\boldsymbol{p}^{\alpha}:\nabla\nabla\delta(\boldsymbol{x}-\boldsymbol{x}^{\alpha}) + \cdots$, (A 2) takes the form

$$\begin{aligned}
&\mu\nabla^2\boldsymbol{u} - \nabla p + \sum_{\alpha=1}^{N}\int_{-L/2}^{L/2} [\boldsymbol{f}^{b}(s; \boldsymbol{x}^{\alpha}, \boldsymbol{p}^{\alpha}) + \boldsymbol{f}'^{\alpha}(s; [\boldsymbol{x}^{\alpha}, \boldsymbol{p}^{\alpha}]; [\boldsymbol{x}^{\beta}, \boldsymbol{p}^{\beta}]_{\beta=1(\beta\neq\alpha)}^{N})]\mathrm{d}s\;\delta(\boldsymbol{x}-\boldsymbol{x}^{\alpha}) \\
&\quad - \sum_{\alpha=1}^{N}\int_{-L/2}^{L/2} \boldsymbol{p}^{\alpha}s[\boldsymbol{f}^{b}(s; \boldsymbol{x}^{\alpha}, \boldsymbol{p}^{\alpha}) + \boldsymbol{f}'^{\alpha}(s; [\boldsymbol{x}^{\alpha}, \boldsymbol{p}^{\alpha}]; [\boldsymbol{x}^{\beta}, \boldsymbol{p}^{\beta}]_{\beta=1(\beta\neq\alpha)}^{N})]\mathrm{d}s\cdot\nabla\delta(\boldsymbol{x}-\boldsymbol{x}^{\alpha}) \\
&\quad + \frac{1}{2}\sum_{\alpha=1}^{N}\int_{-L/2}^{L/2} \boldsymbol{p}^{\alpha}\boldsymbol{p}^{\alpha}s^2[\boldsymbol{f}^{b}(s; \boldsymbol{x}^{\alpha}, \boldsymbol{p}^{\alpha}) + \boldsymbol{f}'^{\alpha}(s; [\boldsymbol{x}^{\alpha}, \boldsymbol{p}^{\alpha}]; \\
&\quad \times [\boldsymbol{x}^{\beta}, \boldsymbol{p}^{\beta}]_{\beta=1(\beta\neq\alpha)}^{N})]\mathrm{d}s:\nabla\nabla\delta(\boldsymbol{x}-\boldsymbol{x}^{\alpha}) + \cdots = \boldsymbol{0}. \qquad \text{(A 3)}
\end{aligned}$$

We note that $\nabla \sim O(k)$, so successive terms in the series on the right-hand side are smaller by $O(kL)$, where k^{-1} ($\gg L$) is the length scale on which the averaged fields in the continuum description are expected to vary (see below); for instance, in the context of a stability analysis, k^{-1} may be regarded as the wavelength of an imposed velocity disturbance. Retaining the first two terms on the right-hand side, with the

second representing the first moment of the bacterial force density, one obtains

$$\mu\nabla^2\boldsymbol{u}-\nabla p+\sum_{\alpha=1}^{N}\int_{-L/2}^{L/2}[\boldsymbol{f}^b(s;\boldsymbol{x}^\alpha,\boldsymbol{p}^\alpha)+\boldsymbol{f}'^\alpha(s;[\boldsymbol{x}^\alpha,\boldsymbol{p}^\alpha];$$
$$\times[\boldsymbol{x}^\beta,\boldsymbol{p}^\beta]_{\beta=1(\beta\neq\alpha)}^{N})]\mathrm{d}s\,\delta(\boldsymbol{x}-\boldsymbol{x}^\alpha)-\nabla\cdot\left[\sum_{\alpha=1}^{N}\int_{-L/2}^{L/2}\boldsymbol{p}^\alpha s[\boldsymbol{f}^b(s;\boldsymbol{x}^\alpha,\boldsymbol{p}^\alpha)+\boldsymbol{f}'^\alpha(s;[\boldsymbol{x}^\alpha,\boldsymbol{p}^\alpha];\right.$$
$$\left.\times[\boldsymbol{x}^\beta,\boldsymbol{p}^\beta]_{\beta=1(\beta\neq\alpha)}^{N})]\mathrm{d}s\,\delta(\boldsymbol{x}-\boldsymbol{x}^\alpha)\right]=\boldsymbol{0}. \tag{A 4}$$

Since the bacteria are force free, the first term on the right-hand side, involving an integral of the force density on each bacterium, is identically zero. Further, each bacterium being torque free, the antisymmetric first moment of the force density is also zero. Note that the bacteria are not merely force free and torque free on average; these conditions hold for each and every configuration. One then obtains, in their final form, the equations governing the motion of the suspending fluid for a given bacterial configuration

$$\mu\nabla^2\boldsymbol{u}-\nabla p-\nabla\cdot\left[\sum_{\alpha=1}^{N}\int_{-L/2}^{L/2}[(s\boldsymbol{p}^\alpha)\boldsymbol{f}^b(s;\boldsymbol{x}^\alpha,\boldsymbol{p}^\alpha)+\boldsymbol{f}^b(s;\boldsymbol{x}^\alpha,\boldsymbol{p}^\alpha)(s\boldsymbol{p}^\alpha)]\mathrm{d}s\,\delta(\boldsymbol{x}-\boldsymbol{x}^\alpha)\right.$$
$$+\sum_{\alpha=1}^{N}\int_{-L/2}^{L/2}\left[(s\boldsymbol{p}^\alpha)\boldsymbol{f}'^\alpha\left(s;[\boldsymbol{x}^\alpha,\boldsymbol{p}^\alpha];[\boldsymbol{x}^\beta,\boldsymbol{p}^\beta]_{\beta=1(\beta\neq\alpha)}^{N}\right)\right.$$
$$\left.\left.+\boldsymbol{f}'^\alpha\left(s;\boldsymbol{x}_\alpha,\boldsymbol{p}_\alpha;[\boldsymbol{x}^\beta,\boldsymbol{p}^\beta]_{\beta=1(\beta\neq\alpha)}^{N}\right)(s\boldsymbol{p}^\alpha)\right]\mathrm{d}s\,\delta(\boldsymbol{x}-\boldsymbol{x}^\alpha)\right]=\boldsymbol{0}. \tag{A 5}$$

We now define the averaging operation as $\langle.\rangle=(1/N!)\int\Omega_N(C_N,t)\mathrm{d}C_N$, where $\Omega_N(C_N,t)$ is the N-bacteria probability density function in phase space at time t, and we have used the abbreviated notation $C_N\equiv[\boldsymbol{x}^\alpha,\boldsymbol{p}^\alpha]_{\alpha=1}^{N}$ for the configuration of N bacteria; this evidently implies the normalization $\int\Omega_N\mathrm{d}C_N=N!$. Averaging (A 5), and noting that the ensemble average commutes with the spatial derivatives, one then obtains

$$\mu\nabla^2\langle\boldsymbol{u}\rangle-\nabla\langle p\rangle-n\nabla\cdot\left[\sum_{\alpha=1}^{N}\int_{-L/2}^{L/2}\int\mathrm{d}\boldsymbol{p}^\alpha\Omega(\boldsymbol{x},\boldsymbol{p}^\alpha,t)[(s\boldsymbol{p}^\alpha)\boldsymbol{f}^b(s,\boldsymbol{p}^\alpha)+\boldsymbol{f}^b(s,\boldsymbol{p}^\alpha)(s\boldsymbol{p}^\alpha)]\mathrm{d}s\right]$$
$$\times\left(\frac{1}{N!}\int\Omega_{N-1|1}(C_{N-1},t|[\boldsymbol{x},\boldsymbol{p}^\alpha])\mathrm{d}C_{N-1}\right)-n\nabla\cdot\left\{\sum_{\alpha=1}^{N}\int_{-L/2}^{L/2}\int\mathrm{d}\boldsymbol{p}^\alpha\Omega(\boldsymbol{x},\boldsymbol{p}^\alpha,t)\,[(s\boldsymbol{p}^\alpha)\right.$$
$$\times\left(\frac{1}{N!}\int\Omega_{N-1|1}(C_{N-1},t|[\boldsymbol{x},\boldsymbol{p}^\alpha])\boldsymbol{f}'^\alpha(s;\boldsymbol{x},\boldsymbol{p}^\alpha;C_{N-1})\,\mathrm{d}C_{N-1}\right)$$
$$\left.+\left(\frac{1}{N!}\int\Omega_{N-1|1}(C_{N-1},t|[\boldsymbol{x},\boldsymbol{p}^\alpha])\boldsymbol{f}'^\alpha(s;\boldsymbol{x},\boldsymbol{p}^\alpha;C_{N-1})\,\mathrm{d}C_{N-1}\right)(s\boldsymbol{p}^\alpha)\right]\mathrm{d}s\right\}=\boldsymbol{0}, \tag{A 6}$$

where we have used the relation $\Omega_N(C_N,t)=n\Omega(\boldsymbol{x}^\alpha,\boldsymbol{p}^\alpha,t)\Omega_{N-1|1}(C_{N-1},t|[\boldsymbol{x}^\alpha,\boldsymbol{p}^\alpha])$, $\Omega_{N-1|1}$ being the probability density function conditioned on one bacterium having a specified configuration. Using the normalization for the conditional probability density viz $\int\Omega_{N-1|1}\mathrm{d}C_{N-1}=(N-1)!$, and assuming that the bacteria are homogeneously distributed over an infinitesimal continuum volume element, one observes that the terms in the summations over α in (A 6) do not depend on the particular bacteria

whose configuration is specified. Equation (A 6) then takes the form

$$\mu\nabla^2\langle\boldsymbol{u}\rangle - \nabla\langle p\rangle - n\nabla\cdot\left[\int_{-L/2}^{L/2}\int \mathrm{d}\boldsymbol{p}\,\Omega(\boldsymbol{x},\boldsymbol{p},t)[(s\boldsymbol{p})\boldsymbol{f}^b(s,\boldsymbol{p})+\boldsymbol{f}^b(s,\boldsymbol{p})(s\boldsymbol{p})]\mathrm{d}s\right]$$
$$-n\nabla\cdot\left\{\int_{-L/2}^{L/2}\int \mathrm{d}\boldsymbol{p}\,\Omega(\boldsymbol{x},\boldsymbol{p},t)\left[(s\boldsymbol{p})\left(\frac{1}{(N-1)!}\int \Omega_{N-1|1}(C_{N-1},t|\right.\right.$$
$$\times[\boldsymbol{x},\boldsymbol{p}])\boldsymbol{f}'(s;\boldsymbol{x},\boldsymbol{p};C_{N-1})\,\mathrm{d}C_{N-1}\Bigg) + \left(\frac{1}{(N-1)!}\int \Omega_{N-1|1}(C_{N-1},t|[\boldsymbol{x},\boldsymbol{p}])$$
$$\left.\left.\times\boldsymbol{f}'(s;\boldsymbol{x},\boldsymbol{p};C_{N-1})\,\mathrm{d}C_{N-1}\right)(s\boldsymbol{p})\right]\mathrm{d}s\right\} = \boldsymbol{0}. \tag{A 7}$$

Defining the conditional average as $\langle.\rangle_1 = (1/(N-1)!)\int \Omega'_{N-1|1}(C_{N-1},t|[\boldsymbol{x},\boldsymbol{p}])\,\mathrm{d}C_{N-1}$, (A 7) may be written in a more compact form as

$$\mu\nabla^2\langle\boldsymbol{u}\rangle - \nabla\langle p\rangle - n\nabla\cdot\left[\int \mathrm{d}\boldsymbol{p}\,\Omega(\boldsymbol{x},\boldsymbol{p})\int_{-L/2}^{L/2}[(s\boldsymbol{p})\langle\boldsymbol{f}(s,t;\boldsymbol{x},\boldsymbol{p})\rangle_1\right.$$
$$\left.+\langle\boldsymbol{f}(s,t;\boldsymbol{x},\boldsymbol{p})\rangle_1(s\boldsymbol{p})]\mathrm{d}s\right] = \boldsymbol{0}, \tag{A 8}$$

where

$$\langle\boldsymbol{f}(s,t;\boldsymbol{x},\boldsymbol{p})\rangle_1 = \boldsymbol{f}^b(s,\boldsymbol{p}) + \frac{1}{(N-1)!}\int \Omega_{N-1|1}(C_{N-1},t|[\boldsymbol{x},\boldsymbol{p}])\boldsymbol{f}'(s;\boldsymbol{x},\boldsymbol{p};C_{N-1})\,\mathrm{d}C_{N-1}. \tag{A 9}$$

The last term in (A 8) may evidently be written as the divergence of an averaged stress tensor, $\nabla\cdot\langle\boldsymbol{\sigma}^B\rangle(\boldsymbol{x},t)$, with the stress tensor being dependent on the microstructure in the following manner:

$$\langle\boldsymbol{\sigma}^B\rangle(\boldsymbol{x},t) = \int \mathrm{d}\boldsymbol{p}\,\Omega(\boldsymbol{x},\boldsymbol{p},t)\int_{-L/2}^{L/2}[(s\boldsymbol{p})\langle\boldsymbol{f}(s,t;\boldsymbol{x},\boldsymbol{p})\rangle_1 + \langle\boldsymbol{f}(s,t;\boldsymbol{x},\boldsymbol{p})\rangle_1(s\boldsymbol{p})]\,\mathrm{d}s. \tag{A 10}$$

Note that although the equations here have been derived for slender bacteria, the final equations and the expression for the averaged stress tensor are, in fact, valid for a particle of an arbitrary aspect ratio. Thus, the only assumption made in deriving the continuum description defined by (A 8) and (A 9) is an appropriate separation of the microstructural (L) and macroscopic length scales (k^{-1}). The entire microstructural information, including hydrodynamically induced correlations in the positions and orientations of different bacteria is contained in the probability density functions that appear in the definition of the stress tensor. Each of these probability density functions satisfies an appropriate kinetic equation; the equation for $\Omega(\boldsymbol{x},\boldsymbol{p},t)$, in particular, appears in the text (see § 2).

Finally, with reference to the mean-field approximation used in § 2, we note that it is more convenient to divide the conditional probability density in (A 9) into a part that does not depend on the configuration of the given bacterium ($\Omega_{N-1}(C_{N-1},t)$), and a residual part ($\Omega'_{N-1|1}(C_{N-1},t|\boldsymbol{x},\boldsymbol{p})$) that reflects the correlations between the positions and orientations of the given bacterium and the bacteria surrounding it. The former may now be used to define an unconditional average that enters the

mean-field representation. In particular, using this decomposition in (A 9), one may write

$$\langle \boldsymbol{f}(s,t;\boldsymbol{x},\boldsymbol{p})\rangle_1 = \hat{\boldsymbol{f}}^b(s,\boldsymbol{x},\boldsymbol{p}) + \frac{1}{(N-1)!}\int \Omega'_{N-1|1}(C_{N-1},t|[\boldsymbol{x},\boldsymbol{p}])\boldsymbol{f}'(s;\boldsymbol{x},\boldsymbol{p};C_{N-1})\,\mathrm{d}C_{N-1}, \tag{A 11}$$

where $\hat{\boldsymbol{f}}^b = \boldsymbol{f}^b + (1/(N-1)!)\int \boldsymbol{f}'\Omega_{N-1}(C_{N-1},t)\,\mathrm{d}C_{N-1}$ now includes contributions from both an externally imposed flow and the mean field. One may define similar averages for the velocity field and velocity gradient induced by other bacteria, and these enter the governing equation (2.5) for $\Omega(\boldsymbol{x},\boldsymbol{p})$ via terms representing the mean-field convection of probability in position–orientation space.

Appendix B: Evaluation of integrals involving $K(\boldsymbol{p}|\boldsymbol{p}')$ and $G_M(\boldsymbol{p}|\boldsymbol{p}')$ over the unit sphere

Herein, we prove that

$$(k_i\hat{u}_j)\int K(\boldsymbol{p}|\boldsymbol{p}')p'_i p'_j\,\mathrm{d}\boldsymbol{p}' = \left[\frac{(3+\beta^2)\sinh\beta - 3\beta\cosh\beta}{\beta^2\sinh\beta}\right](k_i\hat{u}_j)p_i p_j. \tag{B 1}$$

Using the Maclaurin expansion for the exponential kernel viz $K(\boldsymbol{p}|\boldsymbol{p}') = \beta/(4\pi\sinh\beta)\mathrm{e}^{\beta(\boldsymbol{p}\cdot\boldsymbol{p}')} = \beta/(4\pi\sinh\beta)\sum_{m=0}^{\infty}\frac{\beta^m}{m!}(\boldsymbol{p}\cdot\boldsymbol{p}')^m$, one has

$$(k_i\hat{u}_j)\int K(\boldsymbol{p}|\boldsymbol{p}')p'_i p'_j\,\mathrm{d}\boldsymbol{p}' = (k_i\hat{u}_j)\frac{\beta}{(4\pi\sinh\beta)}\sum_{m=0}^{\infty}\frac{\beta^{2m}}{(2m)!}\{p_{i_1}p_{i_2}\cdots p_{i_{2m}}\} \times \int p'_i p'_j\{p'_{i_1}p'_{i_2}\cdots p'_{i_{2m}}\}\,\mathrm{d}\boldsymbol{p}', \tag{B 2}$$

since the terms involving orientation polyads of odd orders vanish, the integral over the unit sphere being identically zero in these cases. For the even-ordered polyads in (B 2), one has the following identity:

$$\int p_{i_1}p_{i_2}\cdots p_{i_{2m}}d\boldsymbol{p} = 0\frac{4\pi}{1\cdot 3\cdots(2m+1)}\Sigma_{\{i\}}\delta_{i_1i_2}\delta_{i_3i_4}\cdots\delta_{i_{2m-1}i_{2m}}, \tag{B 3}$$

where the summation is over all distinct permutations of the m identity tensors (see Bird *et al.* 1987). Thus, an integral over the unit sphere of an orientational polyad of order $2l$ would involve $(2l)!/(2^l\cdot l!)$ such permutations. Using (B 3) in (B 2), one obtains

$$(k_i\hat{u}_j)\int K(\boldsymbol{p}|\boldsymbol{p}')p'_i p'_j\,\mathrm{d}\boldsymbol{p}' = (k_i\hat{u}_j)\frac{\beta}{(4\pi\sinh\beta)} \times \sum_{m=0}^{\infty}\frac{\beta^{2m}}{(2m)!}\{p_{i_1}p_{i_2}\cdots p_{i_{2m}}\}\frac{4\pi}{1\cdot 3\cdots(2m+3)}\sum_{\{i\}}\delta_{ij}\delta_{i_1i_2}\delta_{i_3i_4}\cdots\delta_{i_{2m-1}i_{2m}}, \tag{B 4}$$

where the inner summation now involves $(2m+2)!/2^{m+1}(m+1)!$ terms. Owing to incompressibility ($\hat{\boldsymbol{u}}\cdot\boldsymbol{k}=0$), only those terms in (B 4) that do not contract the indices i and j are non-zero. Since there are $(2m)!/2^m m!$ terms that involve a contraction of i and j, we have

$$(k_i\hat{u}_j)\int K(\boldsymbol{p}|\boldsymbol{p}')p'_ip'_j\mathrm{d}\boldsymbol{p}' = \frac{\beta}{4\pi\sinh\beta}\sum_{m=0}^{\infty}\frac{\beta^{2m}}{(2m)!}\left[\frac{(2m+2)!}{2^{m+1}(m+1)!}-\frac{(2m)!}{2^m m!}\right] \times \frac{4\pi}{1\cdot3\cdots(2m+3)}(k_i\hat{u}_j)p_ip_j, \quad \text{(B 5)}$$

$$= \frac{\beta^2}{2\sinh\beta}\left[\sum_{m=0}^{\infty}\frac{\beta^{2m+1}}{(2m+3)(2m+1)!}-\sum_{m=0}^{\infty}\frac{\beta^{2m+1}}{(2m+5)(2m+1)!}\right](k_i\hat{u}_j)p_ip_j. \quad \text{(B 6)}$$

It may easily be shown that

$$\sum_{m=0}^{\infty}\frac{\beta^{2m+1}}{(2m+3)(2m+1)!} = \frac{(\beta\cosh\beta-\sinh\beta)}{\beta^2}, \quad \text{(B 7)}$$

$$\sum_{m=0}^{\infty}\frac{\beta^{2m+1}}{(2m+5)(2m+1)!} = \frac{(\beta^3+6\beta)\cosh\beta-(3+\beta^2)\sinh\beta}{\beta^4}. \quad \text{(B 8)}$$

Using the above series identities, (B 6) with some manipulation reduces to the right-hand side of (B 1).

The modified Green's function $G_M(\boldsymbol{p}|\boldsymbol{p}')$, like $K(\boldsymbol{p}|\boldsymbol{p}')$ is again a function of $(\boldsymbol{p}\cdot\boldsymbol{p}')$, and an exactly analogous argument gives relation (3.20).

D L K acknowledges financial support from NSF grant CBET-0730579

REFERENCES

Abramowitz, M. & Stegun, I. A. 1970 *Handbook of Mathematical Functions*. Dover.

Batchelor, G. K. 1970 Slender-body theory for particles of arbitrary cross-section in Stokes flow. *J. Fluid Mech.* **44**, 419–440.

Berg, H. C. 1983 *Random Walks in Biology*, chapter 6. Princeton University Press.

Berg, H. C. January 2000 Motile behaviour of bacteria. *Phys. Today* 24–29.

Bird, R. B., Armstrong, R. C. & Hassager, O. 1987 *Dynamics of Polymeric Liquids*, vol. 1. Wylie.

Brenner, H. & Edwards, D. A. 1993 *Macrotransport Processes*. Butterworth Heinemann.

Chandrasekhar, S. 1961 *Hydrodynamic and Hydromagnetic Stability*, chapter 1. Dover.

Chapman, S. & Cowling, T. G. 1991 *The Mathematical Theory of Non-Uniform Gases*. Cambridge University Press.

Childress, S., Levandowsky, M. & Spiegel, E. A. 1975 Pattern formation in a suspension of swimming micro-organisms: equations and stability theory. *J. Fluid Mech.* **69**, 591–613.

Dombrowski, C., Cisneros, L., Chatkaew, S., Goldstein, R. E. & Kessler, J. O. 2004 Self-concentration and large-scale coherence in bacterial dynamics. *Phys. Rev. Lett.* **93** (9), 098103.

Gradshteyn, I. S. & Ryzhik, I. M. 1965 *Table of Integrals, Series and Products*. Academic Press.

Happel, J. & Brenner, H. 1973 *Low Reynolds Number Hydrodynamics*. Noordhoff International Publishing.

Hernandez-Ortiz, J. P., Stolz, C. G. & Graham, M. D. 2005 Transport and collective dynamics in suspensions of confined swimming particles. *Phys. Rev. Lett.* **95**, 204501.

Hinch, E. J. 1977 An averaged-equation approach to particle interactions in a fluid suspension. *J. Fluid Mech.* **83**, 695–720.

Hinch, E. J. & Leal, L. G. 1972 The effect of Brownian motion on the rheological properties of a suspension of non-spherical particles. *J. Fluid Mech.* **52**, 683–712.

Ishikawa, T., Locsei, J. T. & Pedley, T. J. 2008 Development of coherent structures in concentrated suspensions of swimming model micro-organisms. *J. Fluid Mech.* **615**, 401–431.

Ishikawa, T., Simmonds, M. P. & Pedley, T. J. 2006 Hydrodynamic interaction of two swimming model micro-organisms. *J. Fluid Mech.* **568**, 119–160.

Kim, M. J. & Breuer, K. S. 2004 Enhanced diffusion due to motile bacteria. *Phys. Fluids* **16** (9), L78.

Kim, S. & Karrila, S. J. 1991 *Microhydrodynamics: Principles and Selected Applications.* Butterworth-Heinemann.

Larson, R. G. 1988 *Constitutive Equations for Polymer Melts and Solutions.* Butterworth-Heinemann.

Liao, Q., Subramanian, G., DeLisa, M. P., Koch, D. L. & Wu, Mingming 2007 Quadrupole force field dominates the hydrodynamic interactions of swimming Escherichia Coli. *Phys. Fluids*, **19**(6), 061701–061701-4.

Mackaplow, M. B. & Shaqfeh, E. S. G. 1996 A numerical study of the rheological properties of suspensions of rigid, non-Brownian fibres. *J. Fluid Mech.* **329**, 155–186.

Mackaplow, M. B. & Shaqfeh, E. S. G. 1998 A numerical study of the sedimentation of fibre suspensions *J. Fluid Mech.* **376**, 149–182.

Mackaplow, M. B., Shaqfeh, E. S. G. & Schiek, R. L. 1994 A numerical study of heat and mass transport in fibre suspensions. *Proc. R. Soc. Lond.* A **447**, 77–110.

Mehandia, V. & Nott, P. R. 2008 The collective dynamics of self-propelled particles. *J. Fluid Mech.* **595**, 239–264.

Mendelson, N. H., Bourque, A., Wilkening, K., Anderson, K. R., & Watkins, J. C. 1999 Organized cell swimming motions in *Bacillus subtilis* colonies: patterns of short-lived whirls and jets. *J. Bacteriol.* **181** (2), 600–609.

Pedley, T. J., Hill, N. A. & Kessler, J. O. 1988 The growth of bioconvection patterns in a uniform suspension of gyrotactic micro-organisms. *J. Fluid Mech.* **195**, 223–238.

Rahnama, M., Koch, D. L., Iso, Y. & Cohen, C. 1993 Hydrodynamic translational diffusion in fibre suspensions subject to simple shear flow. *Phys. Fluids* A **5**, 849–862.

Saintillan, D. & Shelley, M. J. 2007 Orientational order and instabilities in suspensions of self-locomoting rods. *Phys. Rev. Lett.* **99**, 058102.

Saintillan, D. & Shelley, M. J. 2008 Instabilities and pattern formation in active particle suspensions: kinetic theory and continuum simulations. *Phys. Rev. Lett.* **100**, 178103.

Shaqfeh, E. S. G. & Koch, D. L. 1988 The effect of hydrodynamic interactions on the orientation of axisymmetric particles flowing through a fixed bed of spheres or fibres. *Phys. Fluids* **31** (4), 728–743.

Simha, A. R. & Ramaswamy, S. 2002 Hydrodynamic fluctuations and instabilities in ordered suspensions of self-propelled particles. *Phys. Rev. Lett.* **89**, 058101.

Soni, G. V., Jaffar Ali, B. M., Hatwalne, Y. & Shivashankar, G. G. 2003 Single particle tracking of correlated bacterial dynamics. *Biophys. J.* **84**, 2634–2637.

Subramanian, G. & Koch, D. L. In press The instability of a suspension of swimming bacteria with and without chemoattractants. *J. Fluid Mech.*

Underhill, P. T., Hernandez Ortiz, J. P. & Graham, M. D. 2008 Diffusive and spatial correlations in suspensions of swimming particles. *Phys Rev. Lett.* **100**, 248101.

Wu, X. & Libchaber, A. 2000 Particle diffusion in a quasi-two-dimensional bacterial bath *Phys. Rev. Lett.* **84**, 3017–3020.

Wu, Mingming, Roberts, J. W., Kim, S, Koch, D. L. & DeLisa, M. P. 2006 Collective bacterial dynamics revealed using a three-dimensional population-scale defocused particle tracking technique. *Appl. Environ. Microbiol.* **72**, 4987–4994.